SURVEY ON MODERN PULSED HIGH POWER LASERS

K.J. Witte
Max-Planck-Institut für Quantenoptik, D-8046 Garching/FRG

1. Introduction

The requirements to be met by lasers for particle acceleration are partially similar to those already known for fusion lasers. The power level wanted in both cases is up to 100 TW or even more. The pulse durations favourable for laser accelerators are in the range from 1 ps to 1000 ps whereas fusion lasers require several ns. The energy range for laser accelerators is thus correspondingly smaller than that for fusion lasers: 1-100 kJ versus several 100 kJ. Due to the availability of highly efficient frequency conversion processes no real preference at present exists for a certain wavelength: iodine (1.3 μm), Nd:glass (1.06 μm), XeCl (.308 μm) or KrF (.248 μm) can all be used as long as the high repetition rate capability is disregarded. The CO_2 laser plays a special role. Whereas it is well suited for the grating, plasma or inverse free electron accelerators it is not attractive any more for fusion due to the production of hot electrons leading to an unacceptable level of target preheating.

The design criteria of lasers meeting the requirements mentioned above will be discussed in the following. The CO_2, iodine, Nd:glass and excimer lasers will be treated in detail. The high repetition rate aspect will not be particularly addressed since for the present generation of lasers the wanted rates of far above 1 Hz are completely out of scope. Moreover, for the demonstration of principle these rates are not needed.

2. Paraxial Wave Equation

This section is a short review on laser theory. Its intention is to show that the output characteristics of a complex high power laser system can indeed be calculated with a precision of about 10 % and are thus not subject to the caprice of fortune.

The paraxial approximation to Maxwell's equation has been proven to be completely sufficient for the description of the phenomena occurring in large laser systems such as amplification, diffraction, absorption, scattering, self focussing and frequency conversion. The derivation of the paraxial wave equation starts from Maxwell's equation from which it is easy to derive the following wave equation (mks units, E electric field in V/m, P volume polarization in As/m^2, c velocity of light in vacuum in m/s, $\varepsilon_o = 8.86 \cdot 10^{-12}$ As/Vm permittivity of free space)

$$\nabla^2 \vec{E} - \frac{1}{c^2} \frac{\partial^2 \vec{E}}{\partial t^2} = \frac{1}{c^2 \varepsilon_0} \frac{\partial^2 \vec{P}}{\partial t^2} + \text{grad div } \vec{E} .$$

The paraxial wave equation is obtained by writing

$$E(x,y,z,t) = \frac{1}{2} \vec{\mathcal{E}}(x,y,z,t) \exp\{i(\omega t - kz)\} + \text{c.c.},$$

$$P(x,y,z,t) = \frac{1}{2} \vec{\mathcal{P}}(x,y,z,t) \exp\{i(\omega t - kz)\} + \text{c.c.},$$

making the slowly varying enveloppe approximation ($\partial^2/\partial z^2$, $\partial^2/\partial t$ of $\vec{\mathcal{E}}, \vec{\mathcal{S}}$ negligible) and by assuming grad div $\vec{E} \cong 0$. The last requirement is the condition that the $\vec{E}$-field must be approximately perpendicular to the propagation direction (z-axis here) /1/. If the retarded time $\tau = t - z/c$ is used as the reference frame one obtains with $c = \omega/k$, $\vec{\mathcal{E}} = \mathcal{E}\vec{e}_y$ and $\vec{\mathcal{S}} = \mathcal{S}\vec{e}_y$ ($\vec{\mathcal{E}}, \vec{\mathcal{S}}$ are assumed to be linearly polarized along the y-direction with unit vector $\vec{e}_y$)

$$\frac{\partial \mathcal{E}}{\partial z} - \frac{1}{2ik}\nabla_\perp^2 \mathcal{E} = \frac{k}{2i\epsilon_0}\mathcal{S}. \tag{1}$$

The corrections to this equation are of the order $f^2 = (\lambda/2\pi w_o)^2$ and $g\lambda$ (g gain). w_o is a characteristic transverse beam dimension (not necessarily the beam diameter). Typically, f^2 is $\leqq 10^{-4}$ and $g\lambda \leqq 10^{-3}$ so that eq. (1) is an accurate laser analysis tool (λ laser wavelength).

2.1 Free Space Propagation

In free space eq. (1) becomes particularly simple since $\mathcal{S} = 0$ holds. Free space propagation is very important to know in high power lasers since due to diffraction resulting from hard edges or due to gain inhomogeneities the intensity profile may become heavily structured in the near field, usually the region where passive elements like lenses, beam splitters etc. or the entrance window of an amplifier are located. In order to avoid material damage the intensity peaks have to be known precisely. Soft aperture or image relaying can be used to minimize the unwanted intensity fluctuations.

There are various ways of solving eq. (1) with $\mathcal{S} = 0$. One method which is now frequently used is based on a 2-dimensional Fourier analysis (plane wave decomposition) represented by the Fourier transform of $\mathcal{E}$ /2/

$$\mathcal{F}\{\mathcal{E}\} = \mathcal{E}_F(z,\tau,a_x,a_y) = \int_{-\infty}^{+\infty}\int \mathcal{E}(x,y,z,\tau)\exp\{-2\pi i(xa_x + ya_y)\}\,dx\,dy \tag{2}$$

and the inverse Fourier transform /2/

$$\mathcal{F}^{-1}\{\mathcal{E}_F\} = \mathcal{E}(x,y,z,\tau) = \int_{-\infty}^{+\infty}\int \mathcal{E}_F(z,\tau,a_x,a_y)\exp\{+2\pi i(xa_x + ya_y)\}\,da_x\,da_y \tag{3}$$

where a_x, a_y are spatial frequencies. $\mathcal{E}_F\,da_x da_y$ is the complex amplitude of a plane wave propagating with direction cosines λa_x, λa_y and $[1-(\lambda a_x)^2-(\lambda a_y)^2]^{1/2}$. If the angular spectrum of the beam ($\mathcal{E}_F$) is not too widely spread, the angle between the $\vec{k}$-vector of an individual plane wave component and the z-axis is approximately given by λa with $a^2 = a_x^2 + a_y^2$.

Introducing eq. (2) into eq. (1) leads to the propagation equation of the angular beam spectrum $\mathcal{E}_F$

$$\frac{\partial \mathcal{E}_F}{\partial z} - i\pi\lambda a^2 \mathcal{E}_F = 0$$

which has the solution

$$\mathcal{E}_F(z,\tau,a) = \mathcal{E}_F(0,\tau,a)\exp(i\pi\lambda a^2 z). \tag{4}$$

Free space propagation is therefore easily carried out by inserting eq. (4) into eq. (3). The formalism is readily handled with numerical methods on computers by using FFT-routines (Fast-Fourier-Transforms). The propagation of a pulse between two amplifiers is thus rapidly calculated (see Fig. 1). In cross section 1 $\mathcal{E}_{F,1}$ is firstly determined from $\mathcal{E}_1$ yielding immediately the spectrum $\mathcal{E}^{in}_{F,2}$ on mirror M (position 2) by means of eq. (4). Going back to the physical space by using eq. (3) the field distribution $\mathcal{E}^{in}_2$ impinging on the mirror is calculated. Losses and phase changes introduced by the mirror can now be taken into account by writing

$$\mathcal{E}_2^{out} = M\,\mathcal{E}_2^{in}$$

where M is the mirror transmission function. Moving to the $\vec{k}$ - space again $\mathcal{E}^{out}_{F,2}$ and $\mathcal{E}_{F,3}$ are obtained from eqs. (2) and (4) and then finally from eq. (3) the field distribution $\mathcal{E}_3$ in the entrance plane of amplifier B. Usually the transverse intensity profile changes along the pulse which then has to be cut in several pieces. Each of these is treated according to the procedure just described. At position 3 they are put together to yield $\mathcal{E}_3$. Even with this additional complexity FFT is much faster than a direct integration of eq. (1).

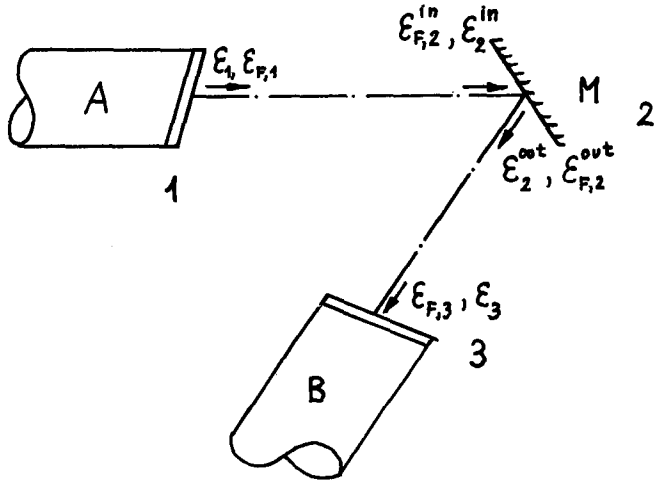

Fig. 1: Free space propagation between two amplifiers.

2.2 Propagation in Polarized Media

Outside free space the polarization $\mathcal{P}$ is not zero and in general nonlinear in the electric field $\mathcal{E}$ so that the Fourier formalism is not favourable any more. It is convenient to distinguish between two cases. In the first only a single wave is present, whereas in the second two or more waves may be present simultaneously.

Single Wave. Here $\mathcal{P}$ can be written as a power series in odd powers of $\mathcal{E}$ according to

$$\mathcal{P} = \epsilon_0 \{ \chi_1 \mathcal{E} + \chi_3 \mathcal{E}^3 + \cdots \} \tag{5}$$

where χ's denote susceptibilities. The real part of χ_1 represents the refractive index, whereas the imaginary part is either exponential loss (Beer's law) or gain as in an amplifier. The term $\chi_3 \mathcal{E}^3$ accounts for two processes. The real part of χ_3 represents self focussing and the imaginary part multiphoton processes.

Two or More Waves. This case includes various processes. Frequency mixing involves the interaction of three waves at different frequencies, ω_1, ω_2 and ω_3 obeying the relation $\omega_3 = \omega_1 + \omega_2$. A special case is second harmonic generation where $\omega_1 = \omega_2$ and thus $\omega_3 = 2\omega_1$ holds; ω_1 is then the pump wave. Frequency conversion is now commonly used in all large fusion laser systems in order to increase the fraction of laser light absorbed by the plasma. Stimulated Brillouin and Raman scattering are also three wave interaction processes with two light waves at frequencies ω_p, ω_s (ω_p pump light, ω_s scattered light) and a sound wave or a molecular vibration, respectively, either at frequency Ω. In laser systems only the Stokes-case is of importance where $\omega_s = \omega_p - \Omega < \omega_p$ holds. The scattered wave amplitude can be made the phase conjugate of the pump wave amplitude if the pump and scattered waves travel in exactly opposite directions (back scattering). Phase conjugation or wave front reversal enables the cancellation of static aberrations acquired by the pulse if the medium in which they occur is traversed first by the pump wave and then by the scattered wave /3/. Phase conjugation can also be achieved by degenerate four wave mixing (DGFW) where the frequencies of the two counter propagating pump waves and the signal and reflected waves are equal. Brillouin, Raman and DFWM-mirrors can also be used for amplifier isolation in order to avoid parasitic chain oscillations and, in addition, to a certain extent for pulse shortening, especially for pulses originally several or more ns long.

Amplification. As already mentioned, the imaginary part of χ_1 is responsible for amplification. For the following discussion it is sufficient to consider only the incoherent approximation, $T_2 \ll T_{pulse}$, where T_2 is the dephasing time and T_{pulse} the pulse duration. In this case the polarization is simply given by (two level system, no detuning)

$$\mathcal{P} = \epsilon_0 \, \mathrm{Im}(\chi_1) \, \mathcal{E} = i \epsilon_0 \Delta N \sigma \mathcal{E} / k \tag{6}$$

where σ is the induced emission cross section at line centre and ΔN the inversion density defined as

$$\Delta N = N_u - \frac{g_u}{g_l} N_l \, . \tag{7}$$

$N_{u,\ell}$ are the population densities of the upper and lower laser levels with the degeneracy factors $g_{u,\ell}$. σ can be calculated from the relation

$$\sigma = \frac{A_{u,\ell}\ \lambda^2}{4\pi^2 n^2\ \Delta\nu} \tag{8}$$

where $A_{u,\ell}$ denotes the Einstein coefficient of spontaneous emission for the transition under consideration, $\Delta\nu$ the medium bandwidth and n the refractive index. If eq. (6) is inserted in eq. (1) and diffraction is neglected in the amplifier which is a reasonable assumption when the amplifier is not too slender ($\frac{d^2}{4\lambda\ell} \geqq 10^2$ with d,ℓ diameter and length of the amplifier) the electric field can be replaced by the intensity

$$I = \frac{1}{2}\,\epsilon_0 c n\, \mathcal{E}\mathcal{E}^* \tag{9}$$

thus yielding the differential equation

$$\frac{\partial I}{\partial z} = (\sigma \Delta N - \gamma) I. \tag{10}$$

Here a loss term γI has been added phenomenologically. For small signal amplification (SSA) ΔN can be considered as constant and the integration of eq. (10) readily yields

$$I(z,\tau) = I(0,\tau)\, \exp\{(\sigma \Delta N - \gamma) z\} \tag{11}$$

whereby $\sigma\Delta N$ is usually referred to as the gain coefficient

$$g = \sigma \Delta N. \tag{12}$$

If medium saturation (large signal amplification, LSA) occurs ΔN is no longer constant and the wave equation must be supplemented by two rate equations for the determination of the population densities $N_{u,\ell}$ of the upper and lower levels. These equations are

$$\frac{\partial I}{\partial z} = (\sigma \Delta N - \gamma) I, \tag{10}$$

$$\frac{\partial N_u}{\partial \tau} = -\sigma \Delta N I/h\nu - \frac{N_u}{\tau_u} + P, \tag{11}$$

$$\frac{\partial N_\ell}{\partial \tau} = +\sigma \Delta N I/h\nu + \frac{N_u}{\tau_{u,\ell}} - \frac{N_\ell}{\tau_\ell}. \tag{12}$$

$h\nu$ is the photon energy, τ_u the actual upper level life time, $\tau_{u,\ell} = 1/A_{u,\ell}$ the life time of the upper level regarding the radiative transition to the lower level and τ_ℓ the actual life time of the lower level. P is the pump rate of the upper laser level ($cm^{-3}s^{-1}$). τ_u is defined by

$$\frac{1}{\tau_u} = \sum_j A_{u,j} + \frac{1}{\tau_q} \tag{13}$$

where $\sum_j A_{u,j}$ counts for radiative transitions from the upper level to lower lying levels and τ_q for non-radiative transitions (quenching). τ_u is an important parameter. It allows for the distinction between storage and non-storage media. For a storage medium the pulse duration T_{pulse} is small compared to τ_u, $T_{pulse} << \tau_u$. CO_2, iodine and Nd are examples of a storage medium. A non-storage medium is characterized by the opposite condition, $T_{pulse} \geq \tau_u$; usually the excimer lasers XeCl and KrF belong to this category when T_{pulse} is in the ns-regime. However, these lasers can also support the propagation of ps-pulses and are then storage lasers ($\tau_u \sim 5$ ns). As it will become clear later the architectures of a storage and a non-storage laser are completely different.

Storage Medium: $T_{pulse} << \tau_u$. We consider a lossless medium with $\gamma = 0$, $T_{pulse} << \tau_{u,\ell}$, τ_ℓ and with $P = 0$ after excitation. Eqs. (11,12) can then be combined to an equation for the inversion density

$$\frac{\partial \Delta N}{\partial \tau} = - \frac{\Delta N I}{e_s} \tag{14}$$

whereby the saturation fluence e_s has been introduced

$$e_s = \frac{h\nu}{\left(1 + \frac{g_u}{g_\ell}\right)\sigma} . \tag{15}$$

If the beam loading exceeds e_s the energy e_{st} (J/ℓ) stored in the medium can be effectively extracted provided the damage threshold of either the laser medium or the output window is nowhere exceeded. In the SSA-case characterized by ($e = \int I dt$ beam fluence)

$$\Delta N \simeq \text{const.}; \; e_{in}, e_{out} << e_s$$

where e_{in}, e_{out} are the beam fluences at the amplifier entrance and exit the relations

$$\begin{aligned} I_{out} &= A_{ss} I_{in} , \\ e_{out} &= A_{ss} e , \\ A_{ss} &= \exp\{\sigma \Delta N \ell\} \end{aligned} \tag{16,a,b,c}$$

hold with A_{ss} being the small signal amplification. The pulse shape is conserved under these conditions. In the LSA-case the integration of the eqs. (10,14) yield the famous Frantz-Nodvik formula /4/

$$e_{out} = e_s \ln\left\{1 + A_{ss}\left(e^{\frac{e_{in}}{e_s}} - 1\right)\right\} . \tag{17}$$

The value of A_{ss} is to be taken prior to extraction. In opposite to the SSA-case strong pulse compression may occur in the LSA-case. The extraction efficiency is determined from

$$\eta_{ex} = \frac{e_{out} - e_{in}}{e_{st}} \leq \frac{1}{1 + g_u/g_\ell} \tag{18}$$

where

$$e_{st} = \Delta N h\nu \tag{19}$$

is the stored energy density, usually measured in J/ℓ. The extraction efficiency comes close to its maximum value $(1+g_u/g_\ell)$ if $e_{in} \geq e_s$ holds.

Non-storage-Medium: Due to $T_{pulse} >> \tau_u$ the time derivatives in eqs. (11,12) can be neglected. If it is further assumed that the lower laser level is practically not populated, $N_\ell \cong 0$, due to its small life time τ_ℓ what is valid for XeCl and KrF the steady state population of the upper level reads

$$N_u = \frac{P\tau_u}{1+I/I_s} \tag{20}$$

whereby the saturation intensity

$$I_s = \frac{h\nu}{\sigma\tau_u} \tag{21}$$

has been introduced. I_s is the counterpart to e_s. The paraxial wave equation can be transformed to

$$\frac{dI}{dz} = \gamma \frac{I/I_s}{1+I/I_s}(I_{Max} - I) \tag{22}$$

where the loss coefficient γ has been retained (necessary for XeCl and KrF) and I_{Max} is the maximum possible intensity achievable by the pulse. I_{Max} reads

$$I_{Max} = I_s\,(g/\gamma - 1) \tag{23}$$

with

$$g = P\sigma\tau_u$$

as the stationary small signal gain. I_{max} is the maximum possible intensity achievable by the pulse. This can be easily seen by realizing that a pulse with an input intensity equal to I_{Max} is not amplified because of dI/dz = 0 so that $I_{out} = I_{in} = I_{Max}$ holds. For $I_{in} > I_{Max}$ the pulse is attenuated since dI/dz is negative. Amplification is thus only possible for $I_{in} < I_{Max}$. When the amplifier is long enough the pulse intensity eventually reaches I_{Max}. The SSA-case, $I << I_s$, has the simple solution

$$I_{out} = I_{in}\,\exp\{(g-\gamma)\ell\} \tag{24}$$

where ℓ denotes the amplifier length. The general solution (LSA-case) of eq. (22) can only be given in an implicit form firstly derived by Schulz-Dubois /5/

$$\left(\frac{I_{out}}{I_{Max}-I_{out}}\right)^\delta \frac{1}{I_{out}} = \left(\frac{I_{in}}{I_{Max}-I_{in}}\right)^\delta \frac{\exp(\gamma\ell)}{I_{in}} \tag{25}$$

with

$$\delta = \frac{1}{1-\gamma/g}\,. \tag{26}$$

The extraction efficiency is defined as

$$\eta_{ex} = \frac{I_{out} - I_{in}}{P\tau_u h\nu l} \,. \tag{27}$$

It is not difficult to see that η_{ex} must have a peak. η_{ex} is zero for $I_{in} = I_{Max} = I_{out}$ and almost zero for the SSA-case, $I \ll I_s$. At some value of $I_{in} < I_{Max}$ η_{ex} must thus show a maximum. For high power excimer amplifiers one typically finds $\gamma l \sim 1$, $\gamma \cong 5\text{x}10^{-3}\,\text{cm}^{-1}$, $g/\gamma \cong 15$, $I_s \cong 2\ \text{MW/cm}^2$ and $I_{Max} \cong 28\ \text{MW/cm}^2$. For an input intensity of $I_{in} = 0.1\ \text{MW/cm}^2$ an extraction efficiency of 40 % is thus possible.

Although the model presented here is a rather simple one it is sufficient for an approximate judgement of the performance of excimer amplifiers. Improvements would result from a more accurate consideration of the kinetics and the V,R dynamics of the various molecules involved.

Amplified Spontaneous Emission (ASE). Due to the radiative life of the upper laser level of only a few nanoseconds amplified spontaneous emission is a serious problem for excimer lasers; in iodine and CO_2 it is of little importance since the Einstein coefficients are much smaller compared to those of KrF or XeCl. Nd:glass is somewhere in between these two extremes; blocking of ASE occurring during the end of the pumping period is usually necessary here to prevent premature target damage.

A rough estimate of the ASE-intensity can be made if one considers a cylindrical amplifier with perfectly absorbing walls so that no reflections have to be taken into account (see Fig. 2). With the inclusion

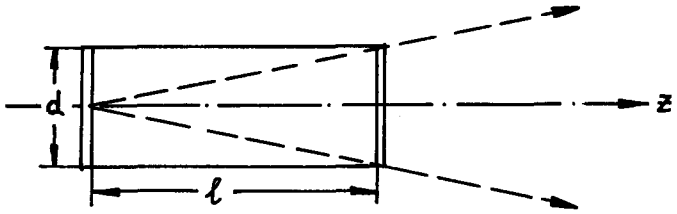

Fig. 2: Beam geometry for an estimation of ASE

of spontaneous emission the paraxial wave equation reads

$$\frac{\partial I}{\partial z} = g I + \frac{N_u h\nu}{\tau_{u,l}} \frac{\delta\Omega}{4\pi} \tag{28}$$

which when integrated on the assumptions g = const., N_u = const. and on the boundary condition I (z = 0) yields

$$I_{ASE} = I(z=\ell) \approx \frac{\delta\Omega}{4\pi} \frac{h\nu}{\sigma\tau_{u,\ell}} \frac{N_u}{\Delta N} \left(e^{g\ell} - 1\right) \simeq \frac{\delta\Omega}{4\pi} \frac{h\nu}{\sigma\tau_{u,\ell}} A_{ss} \,. \tag{29}$$

In eqs. (28,29) $\delta\Omega/4\pi = \frac{(d/\ell)^2}{4\pi}$ is the fraction of spontaneously emitted photons moving in the "right" direction. In eq. (29) the inversion ΔN was set equal to the upper level population density N_u ($N_\ell \sim 0$). It was further required that $A_{ss} >> 1$ holds.

For storage lasers (CO_2, Nd:glass, iodine) the important criterion is that ASE should not damage the target. This may either occur by too much power or energy. The latter can be obtained by the integration of eq. (29) over the pumping time. In any case, the need to avoid premature target damage puts an upper bound on A_{ss} which in a chain is to be understood as the amplification resulting from all amplifiers belonging to the chain. If A_{ss} turns out to be too large saturable absorbers, Pockels cell shutters or Brillouin/Raman mirrors must be introduced in the chain to decrease the ASE gain.

For non-storage media or cw-system, like the long pulse excimer lasers, the main concern is that all the pump power may be converted to ASE and will thus not be available for the pulse to be amplified. In order to prevent this from happening the condition $I_{ASE} < I_s$ must be met or with the help of eqs. (21) and (29)

$$A_{ss} \frac{\tau_u}{\tau_{u,\ell}} \frac{\delta\Omega}{4\pi} < 1. \tag{30}$$

This condition connects the geometry of the amplifier, $\delta\Omega$, with the gain of the medium, A_{ss}. More realistic calculations take wall reflections /6,7/ into account. They show that cuboid-shaped amplifiers have attractive properties.

3. Laser Media

In this section the most important laser medium parameters will be firstly reviewed followed by a presentation of the damage threshold of bare and coated surfaces of various materials and their dependence on wavelength and pulse duration. After that the excitation scheme, performance and overall efficiency achievable in reality will be discussed for the CO_2, iodine, Nd-glass and excimer lasers.

3.1 Survey on Characteristic Laser Medium Properties

In section 2.2 the fundamental properties of a laser medium were introduced. These are wavelength λ, induced emission cross section σ, medium line width $\Delta\nu$, actual upper level life time τ_u, Einstein coefficient $A_{u\ell}$, saturation fluence e_s, saturation intensity I_s, stored energy density e_{st}, inversion ΔN and, for gas lasers, the pressure. These data are collected in Table 1 for the CO_2, iodine, Nd:glass, KrF and XeCl lasers.

Table 1: Laser Medium Properties

Laser Medium	λ μm	σ cm^2	ΔN cm^{-3}	$\Delta\nu$ GHz	$A_{u,\ell}$ s^{-1}	τ_u μs	I_s $\frac{MW}{cm^2}$	e_s $\frac{J}{cm^2}$	e_{st} $\frac{J}{\ell}$	p bar	Ref.
CO_2 *	10.6	6×10^{-19}	6×10^{16}	13	.21	4	/	.23	17	2.4	8
CO_2 **	9.4	1.6×10^{-19}	1.3×10^{17}	75 $>10^3$		.4	/	.70	35	10	9,10
Iodine	1.32	1×10^{-19}	1×10^{17}	20	8	100	/	.5	15	5	11
Nd: glass	1.06	3×10^{-20}	2×10^{18}	10^4	2.800	300	/	5	375	/	12
XeCl †	.308	6.4×10^{-16}	3×10^{14}	5×10^3	9×10^7	5×10^{-3}	.2	1×10^{-3}	~5	5	13,34
KrF #	.248	2×10^{-16}	4×10^{14}	$\sim10^4$	1.4×10^8	4×10^{-3}	1-2	/	10	1-3	6,7

* The data given in this line refer to the 40 kJ/1 ns ANTARES system. $\Delta\nu$ is the width of a single line. The inversion ΔN pertains to the P(20) line only. $e_{st}=(N_{001}-N_{100})\ h\nu$ is the energy difference between the energies stored in the 001 and 100 vibrational modes, thus $\Delta N \cong \mathcal{R}(J)e_{st}/h\nu \cong 0.07\ e_{st}/h\nu$. $\mathcal{R}(J)$ is the rotational partition function. Note that $e_s = h\nu/\{2\sigma\mathcal{R}(J)\} \cong 7\ h\nu/\sigma$ holds.

** In /9/ 3 ps-pulses at 9.4 μm were amplified. 75 GHz is the width of a single line. The R-branch at 9.4 μm has a total width of $> 10^3$ GHz.

\+ The data correspond to the experimental conditions of /34/ where 2 ps-pulses of 300 GHz bandwidth were amplified. σ is the cross section of the 4 main B-X transitions. τ_u is the actual life time of the B-state. e_{st} is the energy difference between the B- and X-states whereas ΔN is the inversion pertaining to the 0-2 transition only (B → X).

\# The data refer to long pulses > 1 ns. Regarding ΔN, e_{st} see footnote for XeCl. σ is a transition averaged cross section.

Together with the pulse duration T_{pulse} the upper level life time τ_u not only determines the type of laser, storage or non-storage, but also the technical realization of the pumping process. The larger τ_u the more economical can the power supply be built. In this sense the short upper level life times of the excimer lasers are somewhat unfavourable.

The Nd-glass laser and the iodine laser are optically pumped. In both cases τ_u is large enough that relatively cheap flashlamp technology can be used. Large volume CO_2 lasers need e-beam sustained discharges. This technique is now rather well understood and established.

Saturation fluence or saturation intensity are important for the extraction efficiency. If they are much smaller than the damage threshold of the various materials occurring in a complex laser system the energy stored in the active medium can be efficiently extracted by the pulse (saturation regime). This is true for the excimer, iodine and CO_2 lasers. Due to the high value of $e_s = 5\ J/cm^2$ only long pulses of several ns duration enable a good energy extraction in Nd:glass lasers; short pulses (< 1 ns) are more or less restricted to the small signal regime with low extraction efficiency.

The column of the stored energy density shows that Nd:glass is the most compact laser system. All the gas lasers roughly need twenty times more volume for the same amount of stored energy. At the first glance this figure is very much in support of glass lasers but falls off importance if it is realized that the amplifiers constitute only a minor fraction of the total volume required by a large laser system.

For gas lasers the pressure determines the strength of the mechanical structure and the thickness of the amplifier windows. Large size amplifiers with a volume of about $1\ m^3$ or more can only tolerate a few bar; high pressure devices as those needed for the generation of ps CO_2-laser pulses can only be built for small volumes of a few liter.

The medium line width $\Delta\nu$ determines the shortest pulse duration which can be realized. Since the pulse bandwidth cannot become larger than $\Delta\nu$, T_{pulse}^{Min} is given by $1/\Delta\nu$ provided the pulse is Fourier-limited. In high pressure CO_2-lasers, in Nd:glass and excimer lasers $\Delta\nu$ is $\geq 10^3$ GHz so that ps-pulses can be amplified. In iodine lasers the shortest pulse duration practically achievable is ~ 50 ps.

3.2 Damage Thresholds

With almost no exception the performance of high power lasers is limited by laser-induced damage occurring either on bare or coated surfaces or within the material supporting the pulse propagation. Since surface damage usually precedes volume damage only surface damage will be considered in the following.

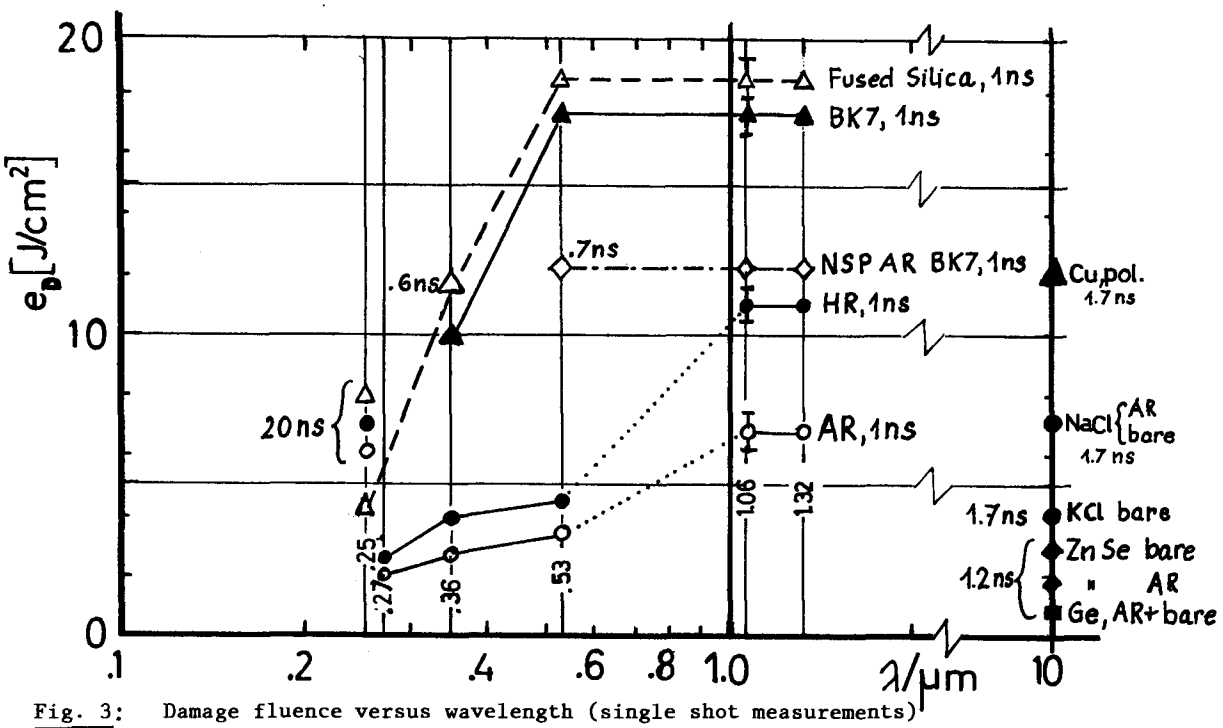

Fig. 3: Damage fluence versus wavelength (single shot measurements)
HR High reflectivity coatings, AR antireflective coatings, NSP AR Neutral-solution processing gradient index AR BK7 surfaces

The morphology of surface damage to transparent dielectric materials indicates that damage is caused by absorption of energy from the laser pulse which heats a small volume of material to the point of stress fracture or melting. Sources of absorption depend on the substrate and coating material and the way they are processed and on the wavelength and pulse width of the laser. The most important mechanisms for damage by pulses in the range of 100 ps to 20 ns duration are absorption by particle impurities of submicron diameter or by small volumes of critical-density plasma generated by avalanche ionisation at impurity sites. Details of the absorption mechanisms are subject of continuing debate and not yet fully clarified. Models used to predict the parametric dependence of the damage threshold on pulse width, wavelength and beam diameter are still at a very early stage. For the purpose of this review article it is sufficient to say that damage is related to impurities and defects rather than to intrinsic properties of the materials.

In Fig. 3 damage threshold data which have been recently published in the literature are collected; the pulse durations are between 0.6 and 20 ns. Measurements are available at 10 μm (CO_2)/14,15/,1.32 μm (iodine), 1.06 μm (Nd), .53 μm, .355 μm, .266 μm and .248 μm (KrF). A large body of the material at the Nd wavelength of 1.06 μm and of its second, third and fourth harmonics as well as that at the KrF wavelength of .248 μm comes from the Lawrence Livermore Laboratory where a big Nd:glass laser program (SHIVA,NOVA) and a smaller KrF laser program is being conducted /16,17,18/. For iodine (1.32 μm) our own measurements have shown (not yet published) that the damage threshold are very much the same as those found for 1.06 μm. Additional data have been found in /12,19,20/.

The largest thresholds are obtained for bare or uncoated surfaces regardless whether they are fused silica, BK7-glass, polished copper, NaCl or KCl. Coated surfaces have a much lower damage threshold. Noticable is the difference between the high reflective (HR) and anti-reflective coatings (AR). The reason for that is not yet clear. Attempts to correlate this phenomenon with the different standing wave field distributions in both cases have not been conclusive. In /16/ it is argued that the higher thresholds of the HR coatings is due to the fact that the interface between the coating and the substrate is not exposed to the laser energy. This is just opposite to the situation occurring in AR coatings where the damage originates at the coating-substrate interface which can be affected by polishing, cleaning and residual surface contamination.

Common to all thresholds is their decrease with decreasing wavelength, especially at short wavelengths. This trend probably results from the increase in absorption at uv-wavelengths of both transparent dielectric materials and common molecular or particulate contaminants.

The neutral-solutions processing gradient index anti-reflective BK7 surfaces (NSP AR BK7) deserve special attention since their damage threshold is even higher than that of HR-coatings /17/. Especially attractive is the independance of the threshold on the wavelength down to .5 µm just opposite to the behaviour of AR-coatings. Unfortunately,

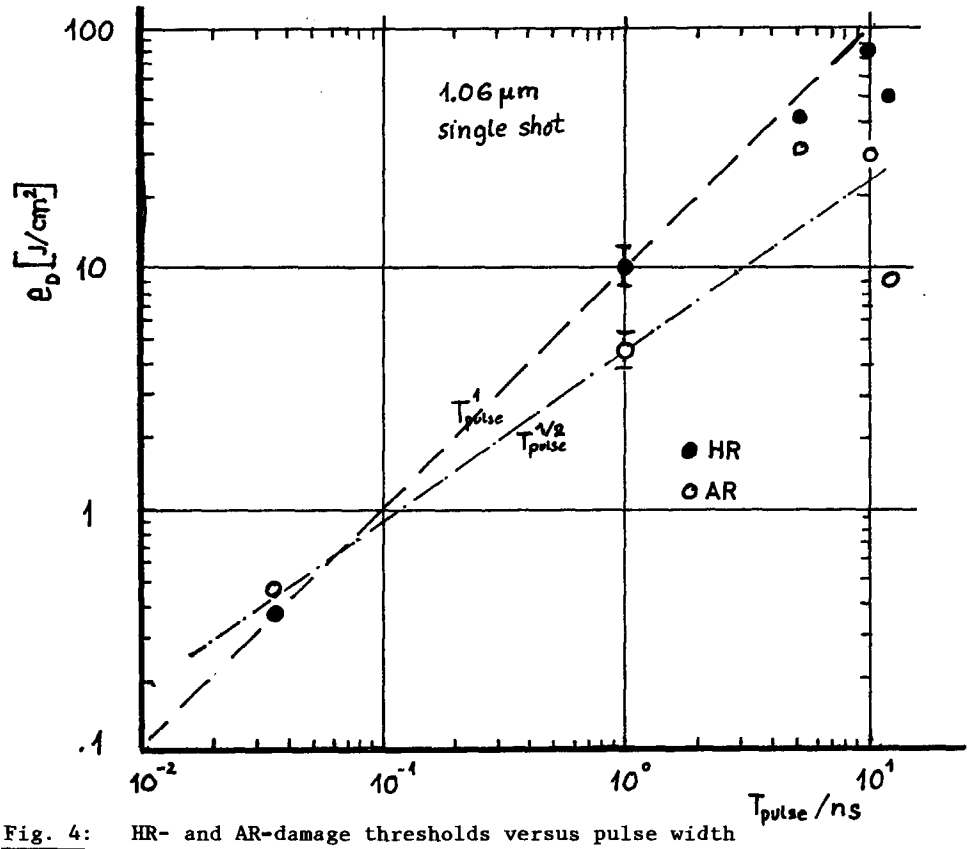

Fig. 4: HR- and AR-damage thresholds versus pulse width

the NSP process does not produce AR surfaces on fused silica which is the only material presently capable of transmitting high intensity pulses below .35 µm. The Sol-Gel Technique /18/ is presently viewed as the most promising method to fabricate porous silica coatings which might have higher damage thresholds than those achievable with AR coatings.

The dependance of the damage threshold on pulse duration is as complex as that on the wavelength. Fused silica and BK7 approximately obey the square root law on the pulse duration

$$e_D \cong \text{const.}\ T_{pulse}^{1/2} \tag{31}$$

in the pulsewidth range from .17 ns to 5 ns /16/ and in the wavelength range from .5 to 1.3 µm. In the UV the exponent (fused silica) appears to be much smaller, .25 versus .5. For HR-and AR-coatings experimental material is only available at 1.06 µm /20/. Fig. 4 shows the damage threshold dependance on T_{pulse} from 35 ps to 12 ns for single shot operation. HR- and AR-coatings appear to follow the square root law only to some extent: $e_D^{HR} \sim T_{pulse}^{0.8}$ and $e_D^{AR} \sim T_{pulse}^{0.7}$. These relations are, however, just a rough estimate, since the data scatter too much at ~ 10 ns. Moreover, the physics responsible for damage at 35 ps is not known and might be different from the mechanisms active at ~ 1ns. The possible role of nonlinear processes such as two photon absorption, harmonic generation or Raman scattering is also not yet identified which all might lower either the reflectivity of HR-coatings or the transmission of AR-coatings and that of the substrate. This field is rather unexplored, especially in the region of ps-pulses.

Finally, it should be pointed out that damage threshold for multiple shot operation are much smaller than those for 1 shot operation. A reduction by a factor of 10 is very likely to occur if the same coating is exposed to $\geq 10^4$ laser shots /20/.

3.3 CO_2 - Laser

The CO_2 level diagram is shown in Fig. 5 /8/. For a typical gas composition of 4:1:1:He:N_2:CO_2 at 1 bar the lifetime of the upper laser level 00°1 is about 8 µs. The main factor in de-exciting this level is CO_2-CO_2 collisions populating other CO_2 excited states. Owing to the Fermi-resonance for the 100-020 levels the equilibration time between them is very short, ~ 4 ns. The complex of levels is then seen to decay to the 01^10 level with a lifetime of ~ .13 µs. The 01^10 level is the "bottle-neck" in the CO_2 laser; in pure CO_2 the lifetime is quite long, ~ 10 µs at a CO_2 pressure of 600 mbar. It has been found that the addition of He to CO_2 preferentially de-excites the 01^10 level, for the cited gas composition the deactivation time is reduced to .2 µs. For pulses longer than a few hundred nanoseconds helium thus improves the extraction efficiency; for operation in the nano- or picosecond regime it has, however, no effect on the extraction efficiency but can be used to control the discharge parameter E/N (E electric field, N molecules per cm^3).

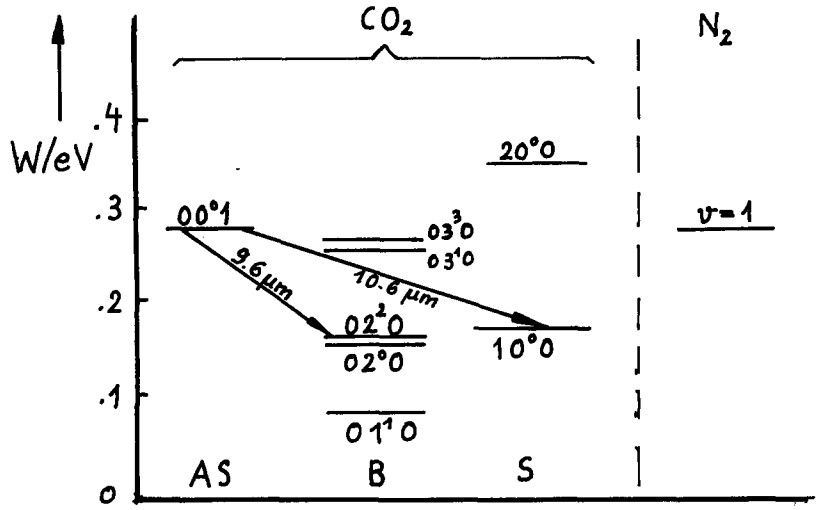

Fig. 5: Energy level diagram of CO_2 and N_2
(AS Asymmetric Stretching Mode, B Bending Mode, S Symmetric Stretching Mode)

Large amplifier volumes can only be pumped by means of e-beam sustained discharges. Self-sustained discharges are inherently unstable and quickly degenerate into constricted, low impedance arcs destroying the electrical and thus optical uniformity of the laser medium. The "trick" of the e-beam controlled discharges relies on the separation of electron production from the electric field which is optimum for the excitation of the CO_2 vibrational level which is due to inelastic e-CO_2, e-N_2 and N_2-CO_2 collisions. The excitation cross sections for CO_2 and N_2 are such that they correlate with different positions of the electron energy spectrum.

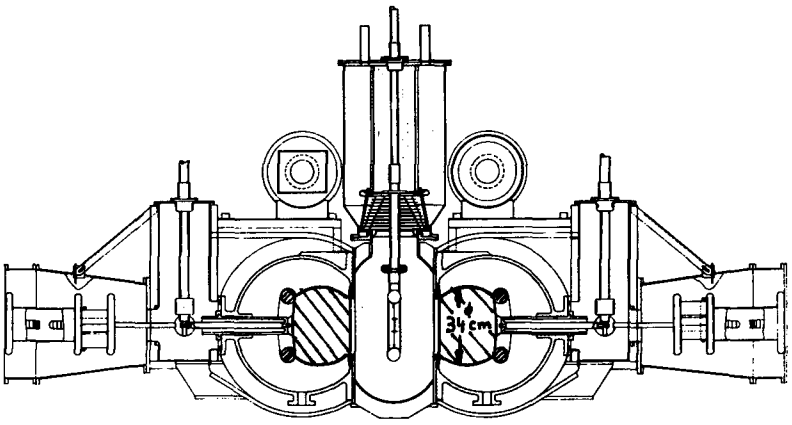

Fig. 6: Cross Section of a HELIOS dual beam module

Fig. 6 is a cross section of one of the four final HELIOS dual beam amplifiers /8,21/. HELIOS is an eight-beam facility delivering altogether 10 kJ in .5 ns into calorimeters. The electron gun is the central assembly suspended from a high voltage vacuum feed through bushing. The cathode structure has a pair of emitter blades on each side of the backing plate and emits a beam of electrons towards thin titanium windows to the left and to the right of the cathode. Each e-beam has a cross section of about 40 x 200 cm^2 and has a current of 5000-7000 A at -300 kV. A rather similar amplifier design is used in the Japanese LEKKO VIII laser system /22/.

The presently biggest CO_2-laser is ANTARES which can deliver an energy of 40 kJ in ~ 1 ns. Fig. 7 shows a photograph of one of the two final modules during the construction period. It clearly demonstrates the enormous size and space requirement of high energy lasers.

The overall efficiency η_{tot} is determined by a product of several fundamental and engineering factors

$$\eta_{tot} = \eta_{ex} \cdot \eta_E \cdot \eta_P \tag{32}$$

where η_p is the pump efficiency, η_{ex} the extraction efficiency and η_E an engineering factor. η_p is defined by /8/

$$\eta_P = \frac{e_{st}}{\int \vec{E} \cdot \vec{j}\, dt} \leq 7\% \tag{33}$$

where $\int \vec{E} \cdot \vec{j} dt$ is the energy input to the laser medium. η_{ex} is calculated from

$$\eta_{ex} = \frac{e_{out} - e_{in}}{e_{st}} \simeq 50\%. \tag{34}$$

Although due to the low value of the saturation energy density the energy stored in the 00°1 vibrational mode can be fairly well extracted, η_{ex} is limited to 50 % since on ns-time scale ground state depletion by helium is ineffective. η_E counts for various engineering limitations resulting from the e-beam generation, pumping power transmission and deposition in the laser medium, incomplete discharge volume utilization, reflection losses of mirrors and windows etc. A reasonable value for η_E is 0.5 so that

$$\eta_{tot} \leq 1.8\%. \tag{35}$$

η_{tot}-values of up to 1.6 % have been achieved in HELIOS.

As already noted, ps-CO_2 lasers need rather large pressure of $\geqq$ 10 bar to achieve a sufficient degree of overlap of the rotational lines. The active volume which can thus be pumped is small; in the devices described in /9,10/ 40 and 32 cm^3 are reported. Under these circumstances a normal discharge with either UV-preionization /9/ or with e-beam preionization /10/ can be used. In /9/ a 2 ps-pulse could be amplified to a power of

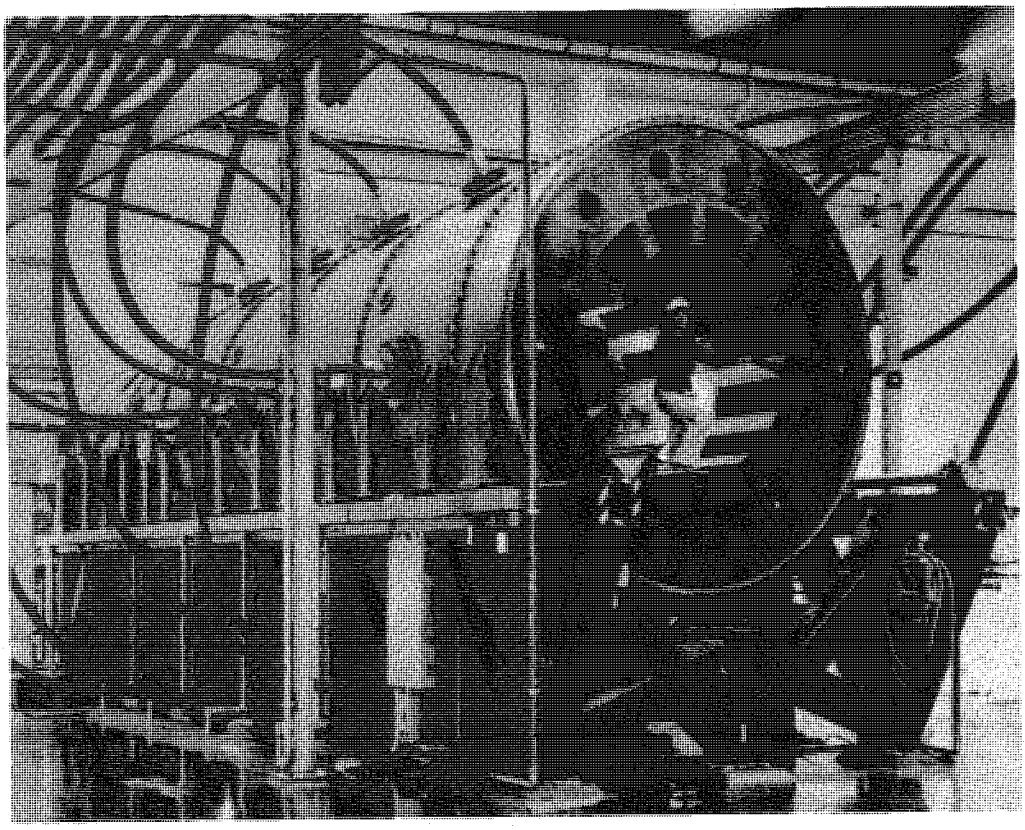

Fig. 7: Final Amplifier Module of ANTARES

10 GW. Hence, if the discharge volume could be scaled to the liter-region which technically appears to be feasible the power level reaches the TW-range thus shortening the gap regarding the power demands of laser grating accelerators.

The generation of ps-CO_2 laser pulses - although straight-forward - requires some effort /9/. It needs a single longitudinal mode CO_2-laser delivering a long output pulse of typically ~ 100 ns duration and a ps-dye laser which is used to switch out a ps-portion from the long CO_2-laser pulse. Switching elements which are activated by irradiation with the dye laser pulse are either polycrystalline CdTe (in reflection) or silicon slabs (in transmission). The power level of the ps-CO_2 pulse achievable with this technique is in the 100 kW-range.

The CO_2 laser is also an interesting candidate for laser plasma accelerators. In this case the pulses don't have to be that short as for laser grating accelerators; durations ~ 50 ps are currently viewed at as an acceptable choice. Such pulses can be effectively generated with the optical free-induction decay /23/. Amplification of 50 ps-pulses needs a medium linewidth of ~ 10 GHz corresponding to a pressure of 2.5 bar. This is just the range in which the high energy amplifiers of ANTARES are operated. This laser is thus

ideally suited as a driver for the plasma accelerator. Since the pulse should have two carrier frequencies (two line operation) amplification has to be controlled in such a way that the two pulse components are intensified by the same amount, i.e. they have to experience the same gain. This requirement puts some restriction on line selection and separation.

3.4 Iodine Laser

Three different pumping mechanisms of the atomic iodine laser radiating at a wavelength of 1.32 µm are known /11/. Two of them are based on the dissociation of fluorinated alkyliodides as CF_3I, C_2F_5I, C_3F_7I etc. either by irridiation with UV-light centred around 270 nm or by electron impact. The third method is chemical pumping and relies on resonant energy transfer between molecular oxygen and atomic iodine according to

$$O_2^*(^1\Delta) + I(^2P_{3/2}) \rightleftharpoons O_2(^3\Sigma) + I^*(^2P_{1/2}) . \tag{36}$$

Chemical pumping is well suited for cw-operation and also for high repetition rate operation. However, its potential for pulsed high-power operation is very limited since the energy is mainly stored in the excited oxygen molecules and too a far less extent in the iodine atoms thus requiring inefficient multiple pass operation for energy extraction.

Dissociation by electron impact produces ground state $^2P_{3/2}$ and excited state $^2P_{1/2}$ iodine atoms with an almost equal amount and is thus not very attractive. Only the photodissociation of fluorinated alkyliodides according to

$$RI + h\nu\,(\sim 270\ nm) \longrightarrow R + I^*(^2P_{1/2}) \tag{37}$$

has proven to generate preferentially excited iodine atoms and is therefore presently the only pumping method used for high power applications. i-C_3F_7I is the most commonly used compound; it has an I*-yield close to 1 and its radical C_3F_7 has a large rate constant for recombination with a ground state iodine atom to the parent molecule C_3F_7I.

Since high energy photons are needed to crack the C-I bonding of the alkyliodides the quantum efficiency of the iodine laser

$$\eta_q = \frac{h\nu_{IR}}{h\nu_{UV}} = \frac{1.5 \times 10^{-19}\,J}{7.2 \times 10^{-19}\,J} = 0.21 \tag{38}$$

is not very high.

The lifetime of the upper, metastable laser level is 125 ms. Actually, due to quenching processes by I_2, RI, CO_2, SF_6, Ar it is much shorter and lies for high power amplifiers between 100 µs and 1 ms depending on the kind of gas mixture used which is composed of C_3F_7I + buffer gas (either Ar, SF_6 or CO_2) with a ratio of RI: buffer gas of 1:50 up to 1:1000 at a total pressure of a few bar /11/.

The detailed spectroscopy of the iodine $^2P_{1/2}$ - $^2P_{3/2}$ transition is of importance for the extraction efficiency. The nuclear spin (I = 5/2) splits the excited state in 2 levels with F_u = 3,2 (see fig. 8) and the ground state in 4 levels with F_ℓ = 4,3,2,1. According to the selection rules $\Delta F = 0, \pm 1$ six transitions (magnetic dipole) are possible; however, under usual conditions, i.e. in the absence of strong magnetic fields, only the 3-4 line which has the highest gain is emitted by an oscillator. The upper state level mixing time is about 30 ns whereas for the ground levels it is much faster, of the order of the dephasing time T_2, ranging from 10 to 60 ps. For a several hundred picosecond or longer pulses the ground state levels can thus be replaced by one level with an effective

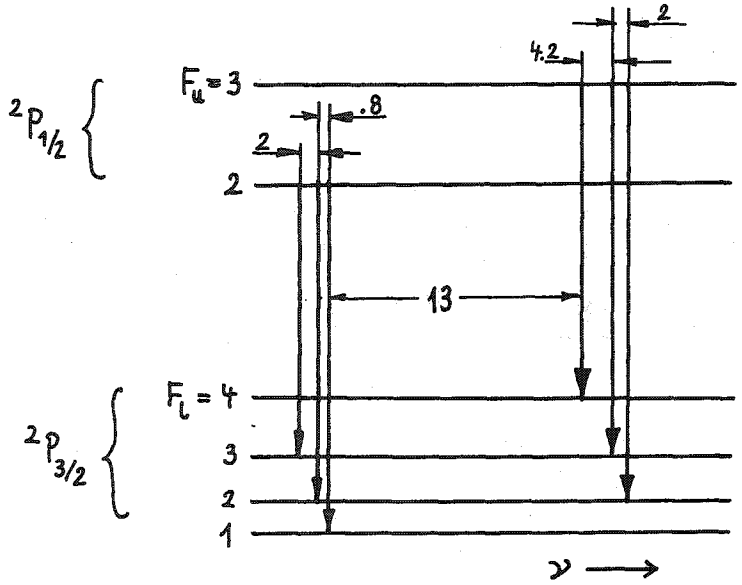

Fig. 8: Hyperfine spectrum of the iodine laser transition (The line separations are in GHz).

degeneracy factor of 24. If the medium linewidth $\Delta\nu$ is $\geq$ 15 GHz (single transition) which is typical for high power amplifiers line overlapping becomes sufficiently strong that a pulse whose carrier frequency is coincident with the centre frequency of the 3-4 transition also has access to the energy stored in the upper F = 2 hyperfine level. In this case the maximum possible efficiency reads

$$\eta_{ex}^{Max} = \frac{1}{1+12/24} = 67\%. \qquad (39)$$

If there is no line overlapping at all ($\Delta\nu \leq 3$ GHz) η_{ex} drops to 45 %. Practically achievable values lie between 50 and 55 % and are connected with strong medium saturation leading to a considerable pulse compression and distortion. This not only means that the chain input pulse duration has to be much longer than that wanted for the exit pulse (up to a factor of 10) but also complicates pulse shaping.

Photodissociation pumping can be done by flashlamps or open discharges. Fig. 9a shows an amplifier based on flashlamp pumping. Pump source and laser medium are completely

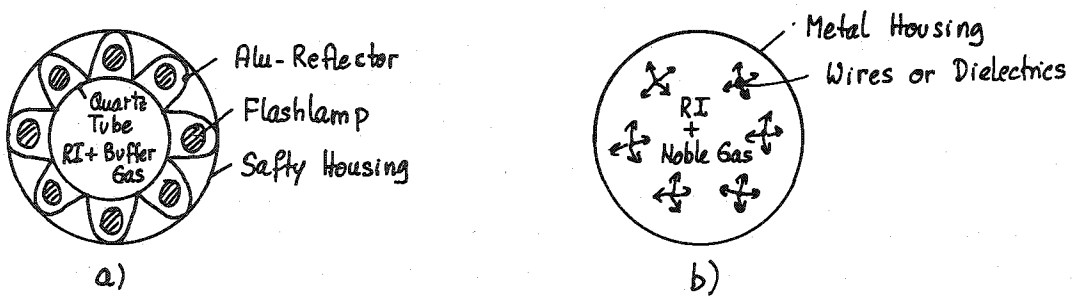

Fig. 9: Amplifier pumped by flashlamps a) or open discharges b)

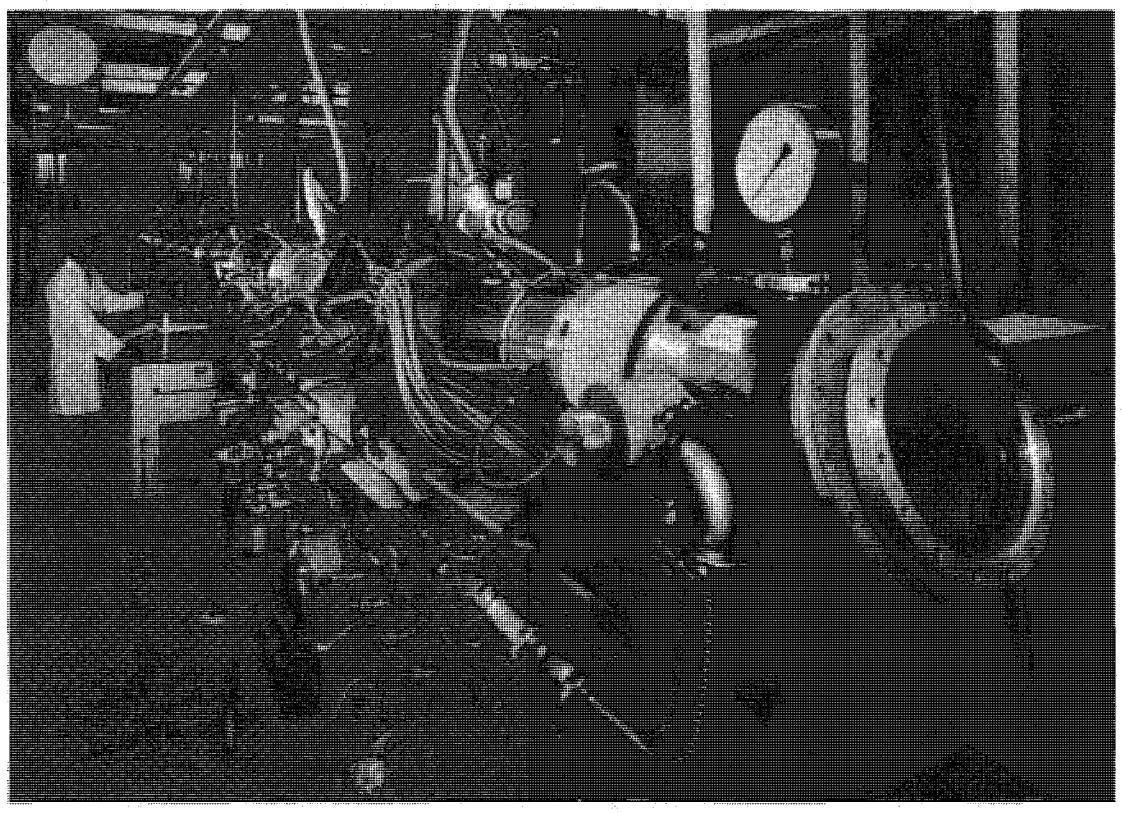

Fig. 10: Final amplifier of the ASTERIX III iodine laser system

separated from each other. With no flashlamps embedded in the laser medium the stored energy density e_{st} scales inversely with the tube diameter d, $e_{st} \sim 1/d$; at d = 30 cm e_{st} = 10 J/ℓ is achievable. For larger diameters external and internal pumping (flashlamps in the laser medium) have to be combined in order to keep e_{st} at a level of 10 J/ℓ.

An alternative to flashlamp pumping is open discharges favoured in russian iodine lasers. An amplifier using this scheme is shown in Fig. 9b. In this case no quartz tubes are needed since the discharge takes place in the laser medium itself. Stored energy densities of up to 20 J/ℓ have been realized for large diameter amplifiers (42 cm).

The advantage of a simple design and a good scalability to large volumes is, however, opposed by the disadvantage of contamination problems; the windows f.e. have to be cleaned after a few shots so that high repetition rate operation is principally difficult to achieve.

The overall efficiency is given by

$$\eta_{tot} = \eta_q \cdot \eta_{ex} \cdot \eta_E \tag{40}$$

where η_E is an engineering factor and counts for flashlamp efficiency (8 % of the energy stored in the capacitors can be converted into UV-light falling in the absorption bandwidth of the fluorinated alkyliodides), optical losses connected with the radiation transfer from the flashlamps to the laser medium and incomplete utilization of the pumped volume. For the present generation of lasers $\eta_E \leq 0.03$ holds. Accepting a value of .5 for η_{ex} the overall efficiency η_{tot} becomes 0.3 % which is to be considered as a kind of upper bound. In the ASTERIX III system /11/ a η_{tot}-value of about .1 % has been realized. Fig. 10 shows a photograph of the final amplifier of the 1-Beam-ASTERIX III-system which can deliver a power of 1 TW at a pulse duration of 250 ps. The repetition rate is 1 shot each 10 minutes.

At a medium linewidth of 20 GHz (single transition) corresponding to an Ar pressure of 5 bar amplification of 50 ps-pulses is possible. Due to the small overall linewidth of only 40 GHz two line operation as required by the beat wave plasma accelerator /24,25/ and characterized by a separation of $> 10^3$ GHz between the two carrier frequencies of the pulse cannot be realized. The iodine laser is thus only useful for that version of the plasma accelerator /24/ which is based upon a pulse with only one carrier frequency.

3.5 Nd:glass Laser (1.06 μm)

Glass has many beneficial properties as a laser host. It can be fabricated in large pieces of variable shape and size (rods up to 11 cm in diameter, disks up to 30 x 60 cm, see Figs. 11,12) with high optical quality and low loss coefficient (0.001 cm^{-1}). It is isotropic, durable and moderate in cost.

Nd goes into the glass as the Nd^{3+} ion each with a different site due to the amorphous glass structure. The absorption and emission lines (see Fig. 13) are therefore inhomogeneously broadened from 20 $cm^{-1} \widehat{=}$ 600 GHz to 200 $cm^{-1} \widehat{=}$ 6000 GHz for the glass as a whole. This permits amplification of short and long laser pulses. In the 24-Beam-

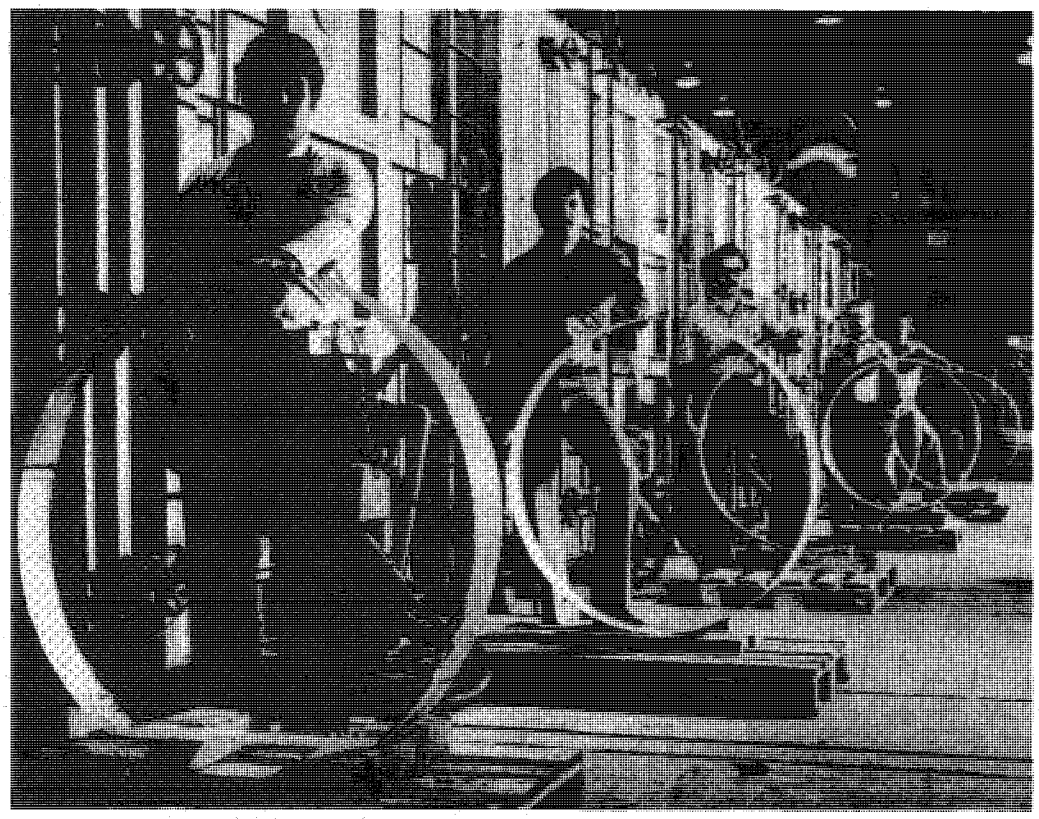

Fig. 11: Large diameter BK7 disks with graded-index antireflective surfaces

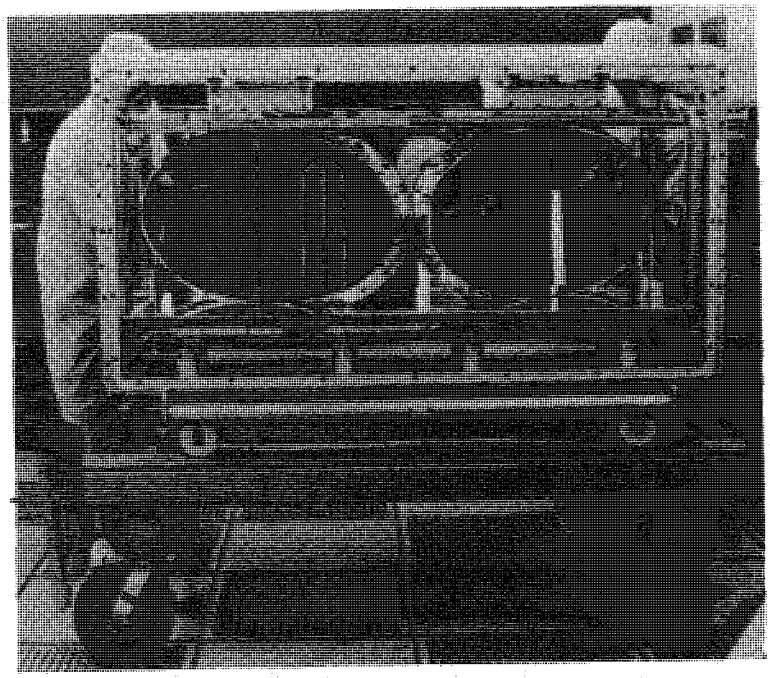

Fig. 12: 46 cm diameter disk amplifier of NOVA

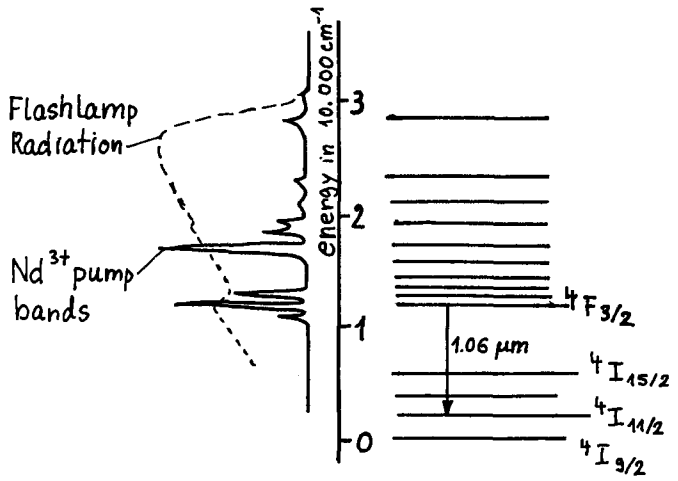

Fig. 13: Absorption spectrum and energy level diagram for Nd^{3+} ions in glass

OMEGA-facility /26/ 50-300 ps-pulses are generated with total powers ranging from 10 TW to 6 TW. The 10-Beam-NOVA-facility /27/, which will be the largest laser in the world after completion by the end of 1984, can amplify pulses with duration from 100 ps to 5 ns with corresponding total powers from 120 TW to 25 TW.

Nd^{3+} ions are optically pumped by flashlamps whose radiation matches the absorption spectrum of the Nd^{3+} ions quite well. Absorbed energy is rapidly accumulated in the $^4F_{3/2}$ atomic levels, which are about 12.000 cm^{-1} above the ground state. These levels have a lifetime of 200 to 700 µs, determined both by radiative and ion-ion non radiative transitions. The dominant fluorescence and highest gain laser action is from the $^4F_{3/2}$ level to the $^4I_{11/2}$ level, which is ~ 2000 cm^{-1} above ground state. Peak gain is at a wavelength from 1.045 to 1.065 µm, depending upon the refractive index of the glass-host composition. The terminal laser level is rapidly depopulated (< 1 ns) and it is far enough above the ground state ($^4I_{9/2}$) that it is thermally almost empty.

At normal doping levels the deposition profile of the pump light in the glass is non-exponential with a characteristic depth of a few cm. This enables a spatially rather uniform excitation which is important for the generation of a beam with a low transverse intensity modulation. The efficiency of transfer from the absorption lines to the upper level $^4F_{3/2}$ is near unity in most glasses. However, the effective energy utilization is η_q ~ 60 % (for a Xenon spectrum) because of the difference between the energy of the absorbing levels and the upper laser level. The lost energy is taken away by phonons heating the glass. 80 % of the energy stored in the capacitor bank is converted to photons by the flashlamps. But not all of these photons are absorbed by the Nd^{3+} ions; the majority goes somewhere else and shows up as heat. Only ~ 3 % is accumulated in the absorbing levels lying above the upper laser level $^4F_{3/2}$. The engineering factor η_E, already introduced when treating the CO_2 and iodine lasers, is thus ~ 0.03. Since the quantum efficiency η_q equals .6 not more than ~ 2 % of the capacitor energy is trans-

ferred into useful inversion of the Nd^{3+} ions. This figure has been found for disk amplifiers and is also approximately valid for rod amplifiers /28/.

At short pulse length of ≦ 100 ps Nd:glass lasers have to be operated in the small signal regime thus showing a low extraction efficiency η_{ex}. Consequently, the overall efficiency $\eta_{tot} = \eta_E \cdot \eta_q \cdot \eta_{EX}$ is also small, fractions of a per mil . Only for long pulses (≧ 1 ns) gain saturation is possible to some extent, yielding η_{tot} values of ≦ .2 %.

Due to its pulse width flexibility, broad amplification bandwidth enabling two line operation with a frequency separation of ~ 10^3 GHz or more and its scalability to very high powers the Nd-glass laser appears to be an appropriate candidate for the plasma and inverse free electron accelerators /29/.

3.6 Excimer Lasers

Excimer lasers like XeCl (308 nm) and KrF (248 nm) have a broad medium linewidth of approximately 5.000 GHz $\widehat{=}$ 1.5 nm thus allowing the amplification of short (ps) and long (ns) pulses as well as two line operation with a frequency separation of up to a few THz. If pumped by e-beams both systems are scalable to large energies; f.e. in /30/ a conceptual design of a 50 kJ KrF amplifier for inertial confinement is presented. The overall efficiency of e-beam pumped excimer lasers is estimated to be at least a few percent and is thus much higher than that of the lasers discussed above. These properties make them interesting candidates both for fusion and particle acceleration.

Up to now the main effort has gone to the KrF laser because its intrinsic efficiency of ~ 12 % (laser output energy over e-beam energy deposited in the laser medium) is approximately twice as high as that of XeCl. This difference has recently become smaller. In /31/ a XeCl laser using an Ar/Xe/HCl mixture achieved an intrinsic efficiency as high as 8 %. Because of its ability to propagate a higher fluence, higher damage thresholds and cheaper optics an XeCl driver system offers significant advantages from a system's viewpoint and has thus become an alternative to an KrF driver.

For large volume amplifiers the pump time has to be several hundred nanoseconds; shorter pump times lead to unattractively expensive devices. Because of the short excited state lifetime of excimer lasers efficient operation is then only possible if energy is extracted during the entire duration of the pump pulse, i.e. the laser pulse has to be as long as the pump pulse. Since fusion needs pulse durations of only a few ns schemes have been devised (see sect. 5.2) allowing a pulse compression from several hundred ns down to some ns. In this case excimer lasers are operated in the non-storage mode.

If the pulse duration is, however, in the ps-range, $T_{pulse} \leqq 50$ ps, excimer lasers have to be treated like storage - lasers, since $T_{pulse} \ll \tau_u$ holds. Pumping times large compared to τ_u can then only be tolerated if the energy is extracted by a series of

ps-pulses separated in time by ~ τ_u. This could be achieved by a modelocked pulse train generated by frequency doubling the output of an appropriately chosen w-modelocked dye laser. For single pulse operation what includes repetition rates up to several KHz the pumping time has to be of the order of τ_u to maintain a reasonable efficiency. This is possible with discharge lasers. Their low intrinsic efficiency of only 1-2 % is, however, offset by their ability to enable repetition rates in the KHz-range. Their most serious limitation arises from the fact that the discharge volume cannot be scaled to large sizes; at present, volumes of ~ 1 liter appear to be an upper bound when uv-preionization is used. However, with the recently developped x-ray preionisation technique /32/ volumes larger by a factor of 10 can be homogeneously pumped without arcing. Moreover, by additionally employing magnetic switching in the electric circuit the power deposition time can be shortened to less than 10 ns /33/. Such a system is ideally suited for amplification of a single ps-pulse.

Recently a ps-pulse was amplified to a power of 20 GW in a conventional uv-preionized XeCl laser /34/. With the new generation of discharge lasers this result can be scaled to the TW-level. This is still not quite that what is wanted, but nevertheless a big step forward. It appears conceivable that with further work it may be possible to gain another factor of 10 what would then be sufficient to reach the 100 TW-level with a 10-beam facility.

In the following the XeCl laser will be treated first. Emphasis will be on the aspects connected with the amplification of ps-pulses (storage mode). For the KrF-laser the non-storage mode of operation will be mainly dealt with.

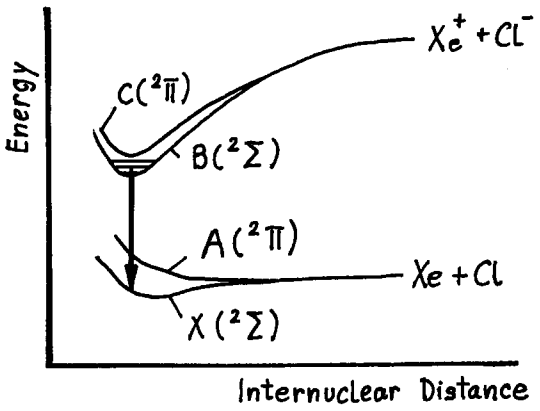

Fig. 12: Schematic potential energy diagram of XeCl

Xenon-chloride (308 nm): The kinetics of XeCl like that of all excimers are rather complicated and will not be discussed here (for details see, f.e. /35/). In high pressure mixtures of Ne, Xe, HCl (typically 4.5 bar Ne, 20 mbar Xe, 4 mbar HCl) which are used in

e-beam controlled and uv-preionized discharges /31,35/ the excited XeCl molecule is predominantly formed by ionic recombination

$$Xe^+ + Cl^- + Ne \rightarrow XeCl^* + Ne. \qquad (41)$$

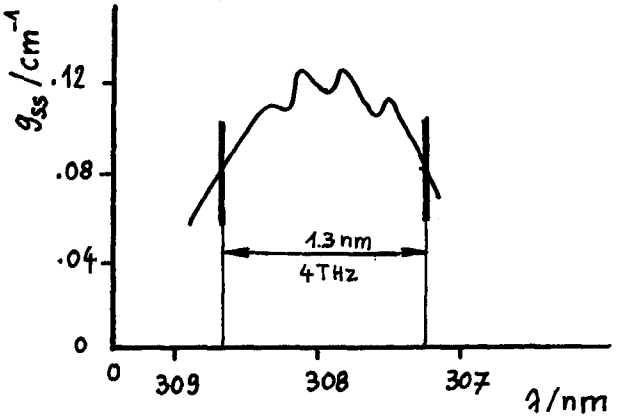

Fig. 13: Spectral gain profile in a He/Xe/HCl/H_2-mixture after /34/

A fast three body charge exchange process produces X_e^+ from N_e^+ which itself is indirectly generated by electrons. Cl^- is formed by dissociative attachment of vibrationally excited HCl.

The ground state of XeCl is covalently bonded /36/ and actually consists of two states (see Fig. 12). Of these, the $^2\Sigma$ has the lowest energy; it forms the ground state and is referred to as the X-state which is weakly bound (255 cm^{-1}). The $^2\pi$ state of the ground state manifold is always repulsive as indicated. Since it is the first state above the ground state it is referred to as the A-state.

The upper laser level is ionically bound and also a manifold with the $^2\Sigma$ state lying lowest. By convention this is referred to as the B-state. The other state is a $^2\pi$ state and is usually designated with C.

The emission spectrum consists of several bands. The strongest band is assigned to the $B(^2\Sigma) \rightarrow X(^2\Sigma)$ transition and gives rise to the laser transition observed to date. All other bands are weaker by at least a factor of ten and are of no importance here. Fig. 13 shows the spectral gain profile of XeCl in a mixture of 3 bar He, 4 mbar H-Cl, 20 mbar Xe and 1.3 mbar H_2. Four bands due to the transitions between the v' = 0 vibrational level in the B-state and v" = 0,1,2 and 3 vibrational levels in the X-state are clearly resolved. It is clear from Fig. 13 that XeCl has sufficient bandwidth for amplification of ps-pulses. In fact, amplification bandwidth-limited pulses as short as ~ .15 ps should be possible, provided that it is bandwidth and not dispersion or something else that

imposes a lower limit on the pulse duration. Fig. 13 also shows that two line operation with the two carrier frequencies separated by 1.3 nm ≙ 4 THz is possible at an equal and reasonable gain for the two components.

The asymmetric structure of the vibrational bands shown in Fig. 13 is due to rotational transition. It is, however, very likely that the discrete nature of the rotational lines will have little effect on the small signal gain profile at high pressure due to pressure broadening and isotopic blending.

In /34/ the energy saturation parameter e_s was measured by combining small signal and large signal gain measurements. For 2 ps-pulses with a bandwidth of 1 Å ≙ .3 THz e_s = 1 mJ/cm^2 and from that using the relation $e_s = h\nu/\sigma$ $\sigma = 6.4 \times 10^{-16}$ cm^2 were found. These values are given in table 1 and are valid for the four main lasing transitions. From gain recovery measurements an upper level life time of about 5 ns could be deduced.

One severe problem in all excimer lasers is the control of ASE. For any amplifier, there is a minimum input signal below which ASE, and not the pulse, will dominate the output of the amplifier. There is also a maximum amplifier gain for a given module geometry above which ASE will saturate the gain by parasitic oscillations. This situation is similar to that known from dye lasers. The maximum tolerable gain g of a XeCl amplifier module with length ℓ and diameter d can be estimated from the relation /34/

$$g \lesssim \frac{1}{\ell} \ln \left\{ \frac{1.9 \times 10^{-4} \ell^2 I_s}{d^2} \right\} \tag{42}$$

where I_s is in W/cm^2 and ℓ,d in cm. F.e. with $\ell/d = 20$, ℓ = 80 cm and $I_s = 2 \times 10^5$ W/cm^2 g should be kept smaller than 10 % per cm. For an amplifier chain removal of ASE from the beam is essential. This requires either suitable saturable absorbers and/or spatial filters.

Finally, a few words will be said regarding the generation of ps-pulses. Because of the short B-state life time modelocking is not an appropriate technique. For this reason another, unfortunately rather complicated method has been developped /34,37/. Single ps-pulses are switched out from a synchronously pumped cw-modelocked dye laser, amplified in an excimer-laser pumped dye amplifier chain to high peak powers and then frequency shifted to serve as an input for an excimer amplifier chain. Achieving and maintaining exact synchroism between several excimer lasers, the mode-locker, pulse selector and resonator length stabilizing feedback circuit is thus quite complex. Recently a much easier scheme has been successfully demonstrated /38/ which avoids the synchronisation problem. It consists of two excimer laser heads switched by one thyratron so that the operation is jitterfree and a simple dye laser (not modelocked) pumped by one of the excimer lasers. This dye laser is designed such that it produces a single ps-pulse which is then amplified, frequency doubled to 308 nm and amplified in the second excimer laser.

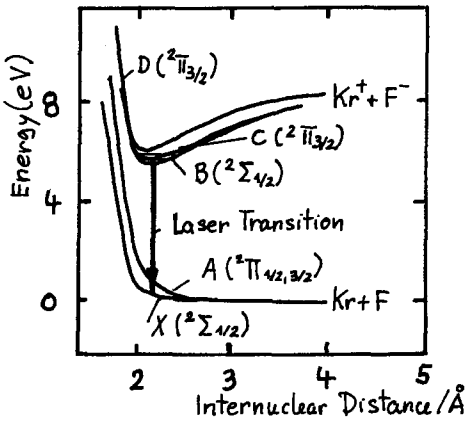

Fig. 14: Potential energy diagram of KrF /36/

Krypton-fluorine (248) nm. Fig. 14 shows the potential energy diagram of KrF which is very similar to that of XeCl except for the fact that the ground state $X(^2\Sigma_{1/2})$ is unbound. The basic kinetics of $Ar/Kr/F_2$ laser mixtures are presently well understood /39/ and will not be repeated here. As already mentioned for large volumes efficient excitation can only be achieved by means of e-beams. The predominant energy transfer is then through the formation of ionic species. In particular, the KrF molecule is formed primarily via the ionic recombination reaction

$$Kr_2^+ + F^- + Ar \longrightarrow KrF^* + Kr + Ar. \qquad (43)$$

The production efficiency η_{KrF} of KrF* can be quite high, up to 25 %, since 65 % of the e-beam energy is converted to ions and excited states finally forming KrF*. There are, however, also losses the major of which are due to spontaneous emission, electron collisional deactivation and photoabsorption. The latter consists of two contributions, saturable and non-saturable losses. The saturable losses mainly arise from Kr_2F trimer formation according to

$$KrF^* + Ar + Kr \longrightarrow Kr_2F^* + Ar. \qquad (44)$$

This represents not only a reduction of the KrF* number density but also a propagation extraction loss because the trimer molecule Kr_2F^* absorbs radiation at 248 nm. This is counteracted to a certain extent by saturation through the action of strong KrF* radiation reducing the KrF* concentration and thus also that of Kr_2F^*. The non-saturable losses result from the absorption of KrF* radiation by F_2, F^- and excited states of the rare gases and are about $5 \times 10^{-3} cm^{-1}$. They limit the output intensity of an amplifier to $\leq 30\ MW/cm^2$. The total photoabsorption losses have the consequence that only 50 % of the energy stored in the KrF* molecules can be converted to excimer radiation, $\eta_{ex} \leq 50$ %.

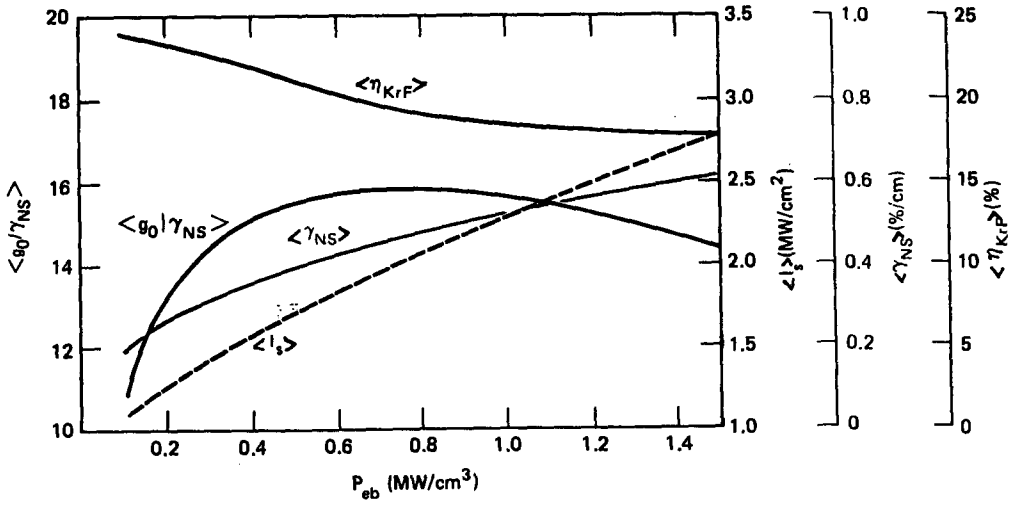

Fig. 15: Dependence of KrF amplifier parameters on e-beam pump power P_{eb} deposited in the medium /7/. η_{KrF^*} is the molecule production efficiency, g_o the small signal gain, γ_{NS} the non-saturable loss coefficient, I_s the saturation intensity. All parameters plotted are average values over fluorine burnout time τ.

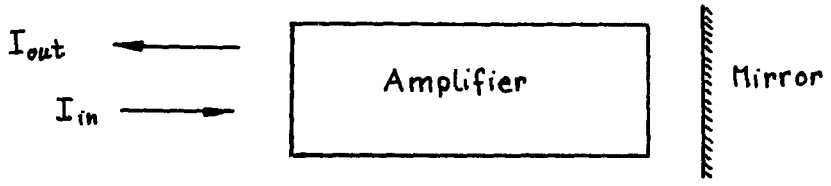

Fig. 16: Bidirectional amplifier

For best laser performance the medium is usually composed of argon (≧ 90 %), krypton (3-8 %) and fluorine (< 1 %) at total pressures between 1 to 3 bar. Fig. 15 shows the characteristics of a mixture consisting of 93.7 % Ar, 6 % Kr and 0.3 % F_2 at a pressure of 1 bar /7/. The laser parameters are average values over the fluorine burn out time τ. This is to be understood in the following sense.

At constant volumetric pump power, P_{eb} (MW/cm^3), deposited in the mixture the laser medium parameters g_o/γ_{NS}, and I_s vary with time. The gain-to-loss ratio g_o/γ_{NS} (NS:Non-saturable losses) changes most rapidly. It at first increases as the KrF* molecule is begun to be formed. However, as time passes by, the F_2 present in the original mixture is depleted by attachment and dissociation kinetic processes. Consequently, g_o/γ_{NS} achieves a maximum and then declines. As the F_2 is consumed, the electron loss mechanism changes from dissociation attachment to dissociative recombination whose rate is slower so that the electron density rises. This changes both the saturation intensity I_s and the non-saturable loss coefficient γ_{NS} as the dominant kinetic processes and composition of the medium change. The usefulness of the medium is determined by the time over which g_o/γ_{NS} remains large. This time period is taken as the fullwidth at 80% of maximum g_o/γ_{NS} and can be considered as a measure of the fluorine burnout time τ. The dependance of τ on the power deposition rate P_{eb} is such that $P_{eb}\tau \cong 0.1\ J/cm^3$ holds for the mixture given above.

Detailed calculations such as those shown in Fig.15 and calculations taking into account finite aperture effects such as parasitic oscillations and ASE (amplified spontaneous emission) show that the bidirectional amplifier (see Fig. 16) is probably an optimum solution. It enables a near uniform fluence gain along the amplifier axis at a sufficiently high level of about 10. Non-saturable losses force tradeoffs between intrinsic efficiency ($= \eta_{KrF^*} \cdot \eta_{ex}$) and energy per aperture. ASE limits extraction efficiency in large aspect ratio amplifiers when the ratio radius over length exceeds a value of 0.15. Parasitic oscillations limit aperture scaling and require diffuse electron beam foil reflectivities ≦ 2 % (current values are ~ 5 %). Achievement of high amplifier energies > 100 kJ within parasitic constraints requires long pump times ≧ 400 ns /6,7/. If parasitic oscillations are controlled, KrF amplifiers appear scalable to an output energy of several hundred kJ at an intrinsic efficiency of ~ 8 % provided the KrF* pulse injected in the amplifier is as long as the e-beam pump pulse (~ 400 ns).

In the western world there are presently two major efforts regarding high power KrF lasers. One is at the Los Alamos Scientific Laboratory/USA where an amplifier module is being constructed whose output energy is expected to be between 10-20 kJ. The other effort is at the Rutherford Appleton Laboratory/England and concerns the high power KrF Laser SPRITE /41/. It is smaller than the LASL-system but more advanced in the sense that experimental results are already available. Fig. 17 shows a cross-sectional view of SPRITE. The laser chamber has a circular cross section. The medium is pumped by by means of 4e-beams. This device has delivered an output pulse of 220 J in 45 ns at a deposited e-beam energy of 2.7 kJ thus yielding an intrinsic efficiency of 8.2 % /41/. The main

efforts are now directed towards solving the problem of pulse compression and associated power multiplication. The aim is to get a 1 ns-pulse with 50 % efficiency, i.e. with an energy ≧ 100 J.

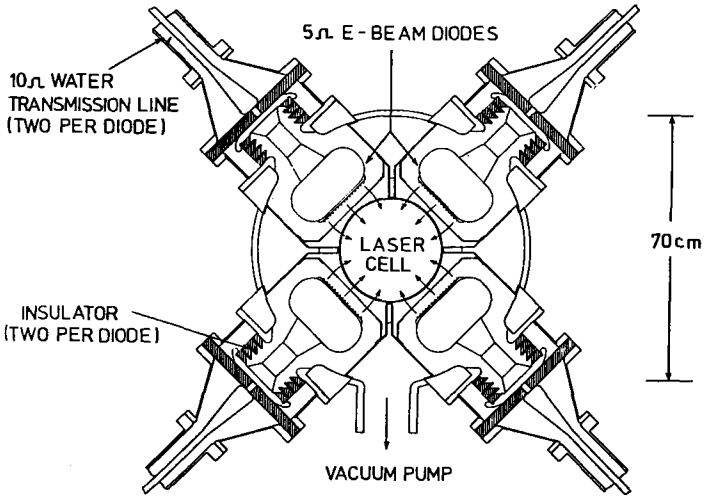

Fig. 17: Cross-sectional diagram of SPRITE

4. Beam Quality

High intensity beams can only be amplified and transmitted over long distances if their angular spectrum is not significantly enlarged upon propagation through the amplifier chain. There is, however, a variety of beam quality impairing processes which will be shortly covered in the following paragraph. The second and third paragraph of this section deals with the cure of these unwanted effects.

4.1 Beam Quality Impairing Process

Optical elements like windows, lenses, mirrors, beamsplitters, polarizers, crystals etc. are not perfect. They have either surface defects such as scratches or attached dust particles or bulk inhomogeneities or both. Since there are many elements of this kind in an amplifier chain it is clear that the beam quality is affected by these inhomogeneities. Moreover, glass plates at Brewster angle put astigmatism on the beam. In addition, there are air paths of 100 m length or even more. Air turbulence - even if it is small - may thus also degrade the beam quality. Processes like scattering, diffraction, non-circular and arbitrary phase variations convert an originally smooth intensity profile to a heavily structured one which is equivalent to a broadening of the angular beam spectrum. This has the unwanted consequence that the beam loading and thus the overall

efficiency cannot be made as large as in the case of a flat profile since otherwise material damage will occur.

Beam quality impairing processes are also possible in the amplifiying medium itself. Of main concern are the deposition of the pump energy, medium saturation and self focusing. If the pump energy is not homogeneously deposited acoustic disturbances are generated since always a significant fraction of the pump energy is directly converted to heat. Another source of such perturbations is the boundary between the pumped and unpumped portions of the laser medium. These problems are mainly encountered in gas lasers with pumping times of about 10 µs or more since the disturbances have then sufficient time to develop and propagate. In the iodine laser these effects limit the pumping time to 10-20 µs. Pumping by e-beams yields a rather uniform medium excitation. Moreover, since the pumping time is usually less than or not more than a few µs acoustic medium perturbations are negligible. This has been verified in e-beam pumped CO_2 and excimer lasers. The acoustic disturbances occurring in high repetition rate discharge lasers do not influence the discharge by which they were generated but perturb the medium for the next following shot when no damping measures are taken. These have turned out to be absolutely necessary if diffraction limited beams are aimed at.

Medium saturation may affect the beam quality in connection with anomalous dispersion. When the carrier frequency ν_p of the pulse does not coincide the centre frequency ν_c of the laser transition and the on-axis portion of the pulse is more strongly amplified than its edges (what is the usual case) the refractive index can be changed in such a way that either focusing or defocusing occurs depending on the relative position of the pulse carrier frequency to the central transition frequency, $(\nu_p - \nu_c) \gtrless 0$. This effect is possible in any of the four high power lasers and needs quantitative consideration when the detuning $\nu_p - \nu_c$ is of the order of the medium linewidth $\Delta\nu$.

Self focusing is a nonlinear process and occurs whenever the refractive index increases with the local intensity of the laser beam according to

$$n = n_0 + n_2 \langle E^2 \rangle = n_0 + \bar{\gamma} I \tag{44}$$

where n_o is the intensity independent part of the refractive index. Thus, the more intense parts of the beam propagate more slowly. An intensity bump on a beam therefore forms a converging lens in the medium, and consequently intensifies itself to a spike. This spike may eventually become so narrow that diffraction balances further self-focusing. However, the involved intensities are so high that any material will be damaged. The filamentation is thus not a feasible solution to the problem of beam propagation.

In order to maintain a good beam quality the bump or ripple growth which is proportional to e^B whereby B is the so-called Beam Break-up Integral /12/

$$B = \frac{2\pi}{\lambda} \int_{chain} \bar{\gamma}(z)\, I(z)\, dz \tag{45}$$

Table 2 : Nonlinear refractive index for various gases and BK7

Medium	Air (1 bar)	Ar (1 bar)	SF_6 (1 bar)	C_3F_7I (10 mbar)	BK7
$\gamma x 10^{10} cm^2/MW$	10	5	10	1	4000

has to be controlled. Catastrophic beam break-up can be avoided if B does not exceed a value of about 3 [12]. Self focusing limits the performance of Nd:glass lasers below pulse duration of 300 ps. Gaseous media suffer less from self focusing than solids (see Table 2). However, at gas pressures of ~ 5 bar and short pulses (≦ 200 ps) self focusing is no longer negligible although not as severe as in glass lasers. This conclusion has been confirmed in the iodine laser ASTERIX III. In ps-excimer lasers no experimental material has been reported so far. Self focusing will certainly become evident when the intensities are further increased. Non-storage excimer lasers are not subject to self-focusing since the involved intensities of ~ 30 MW/cm^2 are too small to cause any appreciable effect. In ns-CO_2 lasers self-focusing is also unimportant since the wavelength is too long. In ps-CO_2 lasers the long wavelength advantage may be offset by the very high beam intensities (> 10^{11} W/cm^2). This conjecture remains, however, to be verified.

Self focusing like the other beam quality impairing processes mentioned above broaden the angular beam spectrum. This is to be understood in the sense that upon propagation more and more beam energy is transferred from the central plane wave component moving along the laser axis to components making a more or less large angle with the laser axis. These components can be removed from the beam by spatial filtering. In case of self focusing this means that after each spatial filter B is reset equal to zero. How such a filter "works", will be explained in the following paragraph.

4.2 Spatial Filtering and Image Relaying

A spatial filter is a combination of two positive lenses separated by the sum of their focal lengths. At their common focus a pinhole of radius R is placed (see Fig.18). Thus only rays having an angle with the filter axis

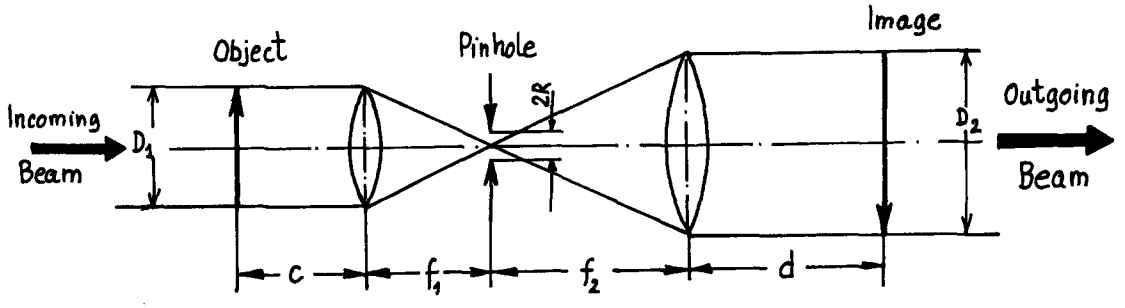

Fig.18: Spatial filter

smaller than R/f_1 (in front of the first lens) will pass through the filter; any other ray will be rejected by the pinhole. In this way a broad angular beam spectrum can be narrowed down so that the intensity profile of the beam emerging from the filter becomes smoother.

A spatial filter is also an image relaying device. An object placed in the front focal plane of the first lens will have its image in the rear focal plane of the second lens. This feature is especially attractive when the "object" is the exit window of an amplifier and the "image" the entrance window of the following amplifier. It is then possible to maintain a smooth intensity profile and thus a good fill factor and high beam loading. However, to understand the image relaying property of the spatial filter more precisely, diffraction must be taken into account.

The electric field distribution $\mathcal{E}_{o,Foc}$ of the object in the common focus of both lenses is given by /2/

$$\mathcal{E}_{0,Foc} = \mathcal{F}\{\mathcal{E}_0\}\,\frac{1}{i\lambda f_1}\exp\left\{\frac{ikr^2}{2f_1}\left(1-\frac{c}{f_1}\right)\right\} \tag{46}$$

where $\mathcal{F}\{\mathcal{E}_0\}$ is the Fourier transform of the object defined by

$$\mathcal{F}\{\mathcal{E}_0\} = \mathcal{F}_0\left\{\frac{x}{\lambda f_1}, \frac{y}{\lambda f_1}\right\} = \iint_{-\infty}^{+\infty}\mathcal{E}_0(x_0, y_0)\exp\left\{-\frac{2\pi i}{\lambda f_1}(x_0x + y_0y)\right\}dx_0\,dy_0$$

with $x^2 + y^2 = r^2$.

Similarly, the electric field distribution $\mathcal{E}_{I,Foc}$ of the image in the common focus of both lenses reads

$$\mathcal{E}_{I,Foc} = \mathcal{F}\{\mathcal{E}_I\}\,\frac{1}{i\lambda f_2}\exp\left\{-\frac{ikr^2}{2f_2}\left(1-\frac{d}{f_2}\right)\right\} \tag{47}$$

with $$\mathcal{F}\{\mathcal{E}_I\} = \mathcal{F}_I\left\{\frac{x}{\lambda f_2}, \frac{y}{\lambda f_2}\right\} = \iint_{-\infty}^{+\infty}\mathcal{E}_I(x_I, y_I)\exp\left\{-\frac{2\pi i}{\lambda f_2}(x_Ix + y_Iy)\right\}dx_I\,dy_I\,.$$

In the pinhole plane the relation

$$\mathcal{E}_{0,Foc}\cdot P_H = \mathcal{E}_{I,Foc} \tag{48}$$

must hold where P_H is the pinhole transmission function. Introducing the magnification factor

$$m = f_2/f_1\,, \tag{49}$$

the "detuning" distance

$$l = (f_1 - c)\frac{f_2^2}{f_1^2} + (f_2 - d) \tag{50}$$

and the new coordinate

$$\xi = r/\lambda f_2 \tag{51}$$

one arrives at a formula relating the Fourier spectrum of the object, $\mathcal{F}_o$, and to that of the image, $\mathcal{F}_I$, in the form

$$\mathcal{F}_I(\xi) = m\, \mathcal{F}_0(m\xi)\, P_H(\xi) \exp\{i\pi\lambda l\xi^2\}\,. \tag{52}$$

In the special case that the "detuning" distance ℓ is zero i.e. the location of the object plane and that of the image plane are related by the laws of geometrical optics and that there is no pinhole, $P_H = 1$ everywhere in the pinhole plane, eq. (51) reduces to

$$\mathcal{F}_I(\xi) = m\, \mathcal{F}_0(m\xi) \tag{53}$$

or transformed back to the physical space

$$\mathcal{E}_I(r_I) = \frac{1}{m}\, \mathcal{E}_0\left(\frac{r_I}{m}\right). \tag{54}$$

Perfect image relaying is thus only possible if the pinhole is removed. If this condition is not met the image will display Gibbs modulation even if the intensity profile in the object plane is smooth. Image relaying and spatial filtering ($P_H = 1$ only in a small area of the pinhole plane, but not everywhere) are thus conflicting claims. In the compromise realized in practice the pinhole diameter 2 R is usually chosen ten times larger than the diffraction limited spot size diameter of the object. This choice only removes those plane wave components from the beam responsible for the worst ripples but has the advantage that image relaying is only weakly blurred by Gibbs modulation. In addition, amplifier isolation is also provided to a certain extent.

4.3 Phase Conjugation

Phase conjugation by stimulated Brillouin-backward scattering (SBBS) was discovered independently by two groups in 1972: in the USSR by Zeldovich, Nosach and coworkers /42,43/ and at Garching by Eidmann and Sigel /44,45/. Zeldovich and Nosach observed phase conjugation using a Ruby laser and CS_2 as the Brillouin-Medium. They already gave a rather detailed explanation of the effect. Eidmann and Sigel found phase conjugation when investigating SBBS from ion-acoustic waves in laser-produced plasmas.

Since then a large body of material has been published /3/. It could be demonstrated that besides SBBS also stimulated Raman or Rayleigh backward scattering (SRaBS, SRayBS) and degenerate four wave mixing (DFWM) can produce phase conjugated waves. Their use in high power laser systems is illustrated in Fig. 19 . A small auxiliary laser illustrates a broad area and some of the scattered light is gathered by the lens and amplified in the

gain medium. The phase conjugation acting like a mirror returns the beam to pass again through the gain medium and onto the target. Any static phase aberrations picked up by the beam on his first passage through the amplifier will be cancelled on his second passage so that the beam hitting the target has perfect quality.

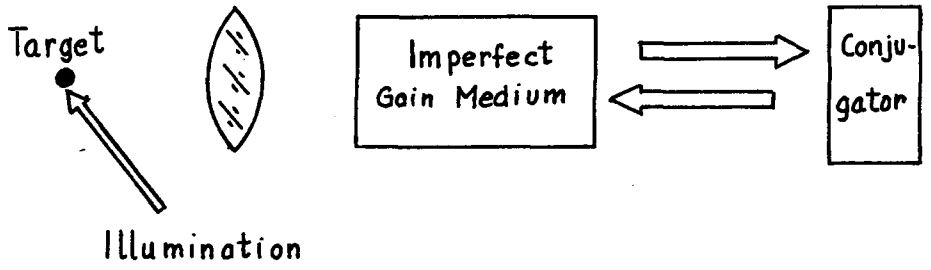

Fig. 19: Laser with phase conjugating mirror

Complete cancellation of static phase aberrations requires zero frequency shift between the incoming and the reflected wave. This is only possible with DFWM. This scheme has, however, the disadvantage that it needs a rather strong pump beam of good beam quality to set up the grating for the reflection of the probe beam. This property together with the low reflection coefficient (relative to the pump beam) makes DFWM not very attractive for an application in a high power laser.

The stimulated backward scattering processes are conceptually much simpler since they don't need additional pump beams. The smallest frequency shift occurs in SRaBS. However, significant phase conjugation has not yet been demonstrated. Many experiments have been reported using either SRaBS or SBBS as the phase conjugating process. The results clearly show that SBBS is superior to SRaBS. SBBS when properly done can produce reflected waves with a high degree of phase conjugation and with reflectivities close to 1. Moreover, the frequency shifts associated with Raman scattering are much larger than those occurring in Brillouin scattering. This is prohibitive for SRaBS when the carrier frequency of the reflected wave falls outside the amplification bandwidth of the amplifying medium.

As already noted, phase conjugation can only cancel static phase aberrations. Wave front distortions resulting from self focusing cannot be compensated. In an amplifying medium the gain must be constant over the beam cross section. If not, the angular beam spectrum is changed upon amplification and this change cannot be canceled by phase conjugation. Wave front perturbations caused by medium saturation are thus not correctable.

Many papers have been published demonstrating the principal ability of SBBS for the correction of wave front distortions occurring in high power laser systems due to thermally induced optical inhomogeneities or poorly fabricated amplifier rods (see f.e. /46/). This should make it possible to reduce the enormous costs of present high power

laser systems substantially since the requirements to be met by the laser materials regarding optical quality can be relaxed.

Besides phase conjugation SBBS and also SRaBS can be used for prepulse suppression and amplifier decoupling since weak pulses experience a very low reflection, $R \leq 10^{-10}$. Another interesting property concerns the ability for significant pulse compression at high efficiency. This can be exploited in non-storage excimer lasers and is currently investigated /41/.

For present research lasers the principle quantity to be minimized in the design process is the ratio of capital cost over focusable output energy or power. The capital cost involve not only those for the mechanical, electrical and optical components but also those for the building and support facilities. This design strategy may lead to the result that the cheapest laser is not that with the highest overall efficiency. Looking at present and projected laser systems a fair estimate of the optimization parameter appears to be 10^3-10^4 DM/J whereby the smaller numbers refer to the larger laser systems. The price of a 1 MJ system could then be expected at a level 10^9 DM. This estimate only holds for long pulse systems (~ 1 ns); for short pulse sytems (~ 1 ps) no cost estimates are available at present.

5. System Design

5.1 Storage Laser Architecture

Large fusion lasers have until now all employed the master-oscillator power-amplifier (MOPA) configuration (see Fig. 20). In MOPA a low-level pulse (usually ~ 1 mJ) is injected in a chain of amplifiers of increasing size and energy. Sizes and gains are adjusted to maintain a fluence level high enough for efficient energy extraction without causing material damage. The MOPA design shown in Fig. 20 is a conceptually simple approach in

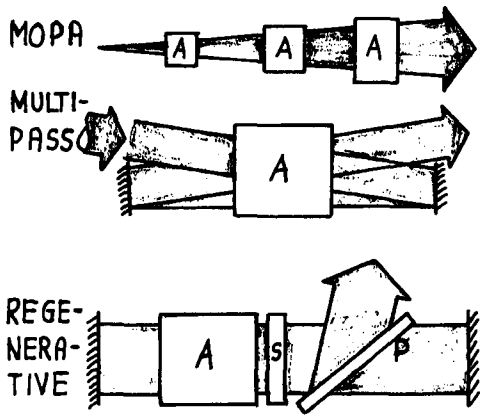

Fig. 20: Three different laser architectures; A amplifier, S switch, P polarizer

the sense that it uses the natural beam divergence for beam expansion so that no beam expanding optics is necessary. An angle of about 1 mrad is required to avoid an excessive chain length. This design is especially convenient for laser media with a low saturation fluence like CO_2 or I since then all the amplifiers except for the very first can be operated in the saturation regime. Very long amplifiers (> 10 cm) should be avoided because the beam divergence of 1 mrad then leads to an incomplete utilization of the pumped volume. A disadvantage of the natural beam divergence concept is that it does not provide for image relaying so that the beam loading is not as close to the damage threshold as it could be.

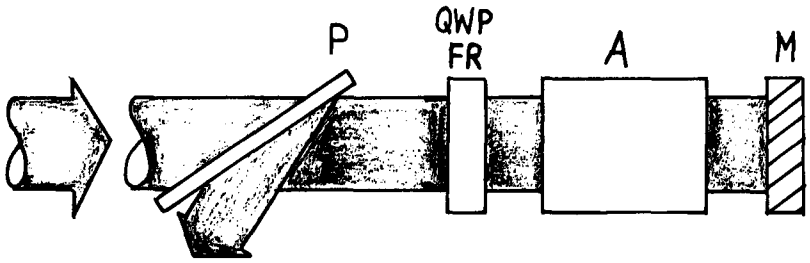

Fig. 21: Double pass amplifier (P polarizer, QWP quarter wave plate, A amplifier, M Mirror: conventional or SBBS

For laser media with a high saturation fluence like Nd the simple MOPA architecture is not as attractive since the chain would have mainly to be operated in the small signal regime. Alternatives are the multipass amplifier and the regenerative amplifier (see Fig. 20). Multipass systems are only technically feasible for short amplifiers. Even in this case long propagation paths are required to reduce beam vignetting at the amplifier aperture. The regenerative amplifier is a larger version of the usual oscillator geometry used for the generation of low power pulses. The major problem in this concept is the requirement for a large diameter optical switch that has a rapid switching time, low leakage (no prepulses) and the need for low-loss optical components. Due to these difficulties the regenerative amplifier concept has not been used so far in a high power system. Similar holds for the multipass amplifier arrangement with the exception of the double pass configuration shown in Fig. 21. Since beam separation is effected by polarization control this configuration is also applicable to long amplifiers. The mirror can be of conventional or SBBS-type. In the first case a saturable absorber or an electrooptic shutter is necessary to avoid parasitic chain oscillations. An advanced MOPA configuration is shown in Fig. 22. By means of expanding telescopes the growth of the beam diameter is optimized to extract energy from the amplifiers in a more efficient way, than it is possible with the simple MOPA arrangement. Moreover, spatial filtering and image relaying can be easily incorporated so that a smooth beam profile and high fill factor can be transported all along the laser chain. Each stage also contains the necessary components for isolation to avoid premature target damage by prepulses, ASE or

parasitic oscillations of the entire chain. When the advanced MOPA architecture is properly designed the beam loading approaches the damage threshold in each stage at a corresponding position or everywhere (isofluence), i.e. in each component of each stage the fluence is at the damage level.

The advanced MOPA architecture is the arrangement for present Nd:glass laser systems like NOVETTE and NOVA and also for the 2 kJ ASTERIX IV system to be put into operation by 1986.

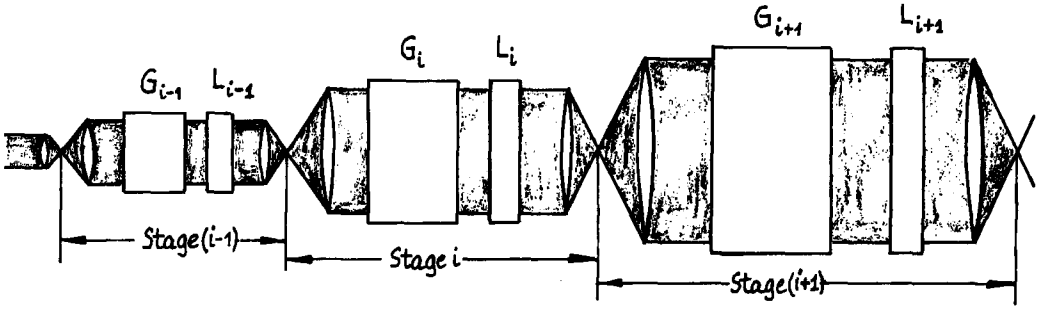

Fig. 22 : Advanced MOPA architecture (G Gain, L loss dur to scattering, reflection, absorption and filtering)

5.2 Non-Storage Laser Architecture

As already pointed out KrF excimer lasers are efficient and scalable to sizes interesting for inertial confinement fusion. The main characteristic is the short excited state life time so that efficient operation is only possible if energy is extracted during the entire duration of the pump pulse of ~ 400 ns duration; shorter pump times are unattractively expensive for large amplifiers. Since fusion requires pulse durations of a few nanoseconds an efficient method for pulse shortening of KrF pulses from 400 ns down to at least 10 ns is necessary.

One technique for this purpose is staged multiplexing shown schematically in Fig. 23 . The large aperture KrF amplifier is e-beam pumped for a time interval of 4 τ and energy is sequentially extracted by two angle encoded

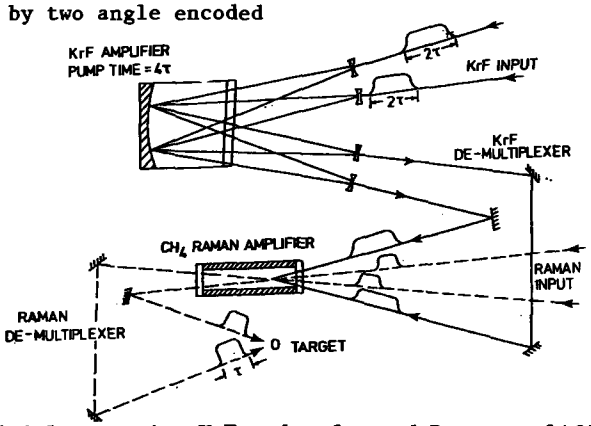

Fig. 23 : 2x2 Staged multiplexer using KrF and a forward Raman amplifier (——— KrF beams, - - - 1st Stokes Raman beams)

KrF laser pulses each of duration 2 τ one delayed from the other by 2 τ. The first KrF pulse enters the amplifier at the start of the e-beam and the second leaves the amplifier at the end of the e-beam. After amplification the two KrF pulses (248 nm) are decoded and appropriately delayed to simultaneously pump a forward Raman amplifier with a pump time of 2 τ. This amplifier is itself optically multiplexed by two pulses of duration τ at a wavelength of 268 nm (corresponding to the Raman shift in CH_4). These two new pulses are then decoded and directed on target in synchronism. A pulse compression factor of 4 has thus been achieved with an intensity gain probably approaching 4 since the conversion efficiency from the pump beam to the stokes beam is close to unity even if both beams travel at an angle to each other. Using this principle a 5 x 12 staged multiplexing scheme is being designed for SPRITE /41/ to compress the expected 60 ns/300 J output pulse into a 1 ns pulse at 268 nm.

A second technique for compressing a long pulse is that of backward wave Raman scattering /47/ whereby also large compression ratios can be achieved. The conversion efficiency is, however, about inversely dependent on the ratio of T_p/T_R where T_p denotes the duration of 248 nm pump pulse and T_R that of the Raman shifted pulse; at $T_p/T_R = 5$ a conversion efficiency of 60 % may be achievable. In spite of this disadvantage combination of backward wave Raman scattering and multiplexing appears to be attractive since then each technique has not to be exhausted up to its technological limits.

A third method is SBBS, as already mentioned. Conceptually it is the simplest of all but not yet fully explored in the sense that its limitations have still to be determined.

In the design of these non-storage systems proper consideration of suppression of prepulses due to ASE or parasitic oscillations is also an important task.

5.3 Optimization

Because the performance of each component in a chain depends on the laser-pulse duration a laser system can only be optimized at one pulse duration. Three regimes of system design can be clearly distinguished: a) the short pulse region below a few hundred picoseconds where self focussing is the limiting process; b) the intermediate regime from a few hundred picoseconds to several nanoseconds where surface damage controls the laser performance and c) the long pulse regime above several nanoseconds where the stored energy determines the laser performance. Short pulse Nd:glass lasers (≦ 100 ps) and short pulse iodine lasers (≦ 200 ps) belong to category a). CO_2 lasers and iodine lasers both operating at ~ 1 ns are examples of category b). The nonstorage KrF laser has a typical pulse duration of several nanoseconds or longer; it is stored-energy limited and thus falls under category c). For ps-CO_2 and excimer lasers the processes limiting the system performance have still to be identified. ps-excimer lasers will probably be stored energy limited.

The optimization procedure starts with the desired laser output energy E and assumes a number of beams M. The output energy per beam or chain is then E/M. The number of stages

per chain is determined by working backwards using as a first approximation the concept of isofluence and obeying the limitations on the small signal amplification such that ASE, prepulses and parasitic oscillations are not harmful to the target. By varying the number of beams and thus the number of stages per chain the design yielding the lowest value for the capital costs per unit focusable output energy can be found. Usually the laser system with the technologically still feasable smallest number of beams, i.e. with large-diameter final stages, minimizes the total costs.

5.4. Isolation

As already pointed out protection of the target from damage due to ASE, prepulses or parasitic oscillations of the amplifiers require a careful isolation of the chain from the oscillator delivering the chain input pulse and from the amplifiers among each other. In addition the chain has to be protected from the light backreflected from the target.

a) Oscillator-Chain: The shutter is usually a polarizer-Pockels cell arrangement. If a mode-locked oscillator is used it also acts as a pulse selecting system. If the oscillator emits a long pulse the shutter simultaneously acts as pulse cutter i.e. it cuts out a short pulse from the long pulse. In any case, however, the contrast ratio of the shutter defined as the ratio of the transmitted intensity to the incident intensity at closed shutter has to be $\sim 10^3$ smaller than the inverse of the effective small signal amplification of the chain. Only then prepulses are kept at a level that they don't damage the target. If the chain input pulse is generated by frequency shifting the pulse from another laser decoupling is perfect.

b) Stage-Stage: Isolation from stage to stage is necessary to avoid parasitic amplifier oscillation and build-up of ASE. Several measures can be taken for this purpose. Saturable absorbers are applied in the CO_2 laser (gas mixtures) and in the iodine laser (dyes or hot iodine cells). Equally well suited are polarizer-Pockels cell arrangements. They are used in Nd, I and KrF lasers, but only for diameters $\leq$ 10 cm. Spatial filtering is also an isolation technique, but of course not as effective as the others already mentioned. SBBS mirrors are especially attractive for KrF (long pulse) and to a certain extent also for iodine; their potential has not yet been fully evaluated.

c) Target Backreflection: For diameters up to 20 cm Faraday rotators are efficient in protecting the chain from the light retroreflected from the target. They are usually placed in front of the final amplifier. This technique has been widely employed in Nd and I and may also be used in KrF. For large diameters (> 20 cm) Faraday rotators become too expensive. Then the plasma shutter is the more favourable solution. It is placed between the chain exit and the target and can be used for any laser.

6. References

/1/ Lax M., Louisell W.M., Mc Knight W.B.: Phys. Rev. A 11, 1365 (1975)

/2/ Goodmann J.W.: Introduction to Fourier Optics. Mc Graw-Hill Book Company, San Francisco - New York - London, 1968

/3/ Optical Phase Conjugation, (ed. R.A. Fisher), Academic Press, New York - London - Toronto, 1983

/4/ Frantz L.M., Nodvik S.J.: J. Appl. Phys. 14 (1963), 2346

/5/ Schultz-Dubois E.O.: Bell System Techn. J. 43, 625 (1964)

/6/ LLL Annual Report UCRL - 50021-78, Vol. 3, Sect. 8, pp. 10-48 (1971)

/7/ LLL Annual Report UCRL - 50021-79, Vol. 3, Sect. 7, pp. 1-45 (1980)

/8/ Singer S., Elliot C.J., Figuereira J., Libermann I., Parker J.V., Schappert G.T.: High-Power, Short-Pulse CO_2 Laser Systems for Inertial-Confinement Fusion. In "Proc. Int. School of Physics Enrico Fermi, Course LXXIV," (ed. C. Pellegrini), North Holland Publishing Company, Amsterdam - New York - Oxford, 1981

/9/ Corkum P.B.: Opt. Lett. 8 (10), 514 (1983)

/10/ Chong-Yi W., Schwab C., Fuss W., Kompa K.L.: Opt. Commun. 46, 311 (1983)

/11/ Brederlow G., Fill E., Witte K.J.: The High Power Iodine Laser, Springer Series in Optical Science, Vol. 34, Springer Verlag, Berlin - Heidelberg - New York, 1983

/12/ Brown D.C.: High Peak Power Nd:Glass Laser Systems, Springer Series in Optical Sciences, Vol. 25, Springer Verlag, Berlin - Heidelberg - New York, 1981

/13/ Maeda M. et al.: Appl. Phys. Lett. 36, 636 (1980)
Reksten G., Varghese T., Bradley D.J.: Appl. Phys. Lett. 38, 513 (1981)

/14/ Carlsson R.L. et al.: IEEE J. Quant. Electron QE-17 (9), 1662 (1981)

/15/ Figueira J., Thomas S.: IEEE J. Quant. ELectron. QE-18 (9), 1381 (1982)

/16/ Lowdermilk W.H., Milam D.: IEEE J. Quant. Electron. QE-17 (9), 1888 (1981)

/17/ LLL Annual Report 82, UCRL-50021-82, section 7, pp. 7.24-7.33

/18/ LLL Annual Report 83, UCRL-50021-83, section 6, pp. 6.31-6.40

/19/ Bennet H., Guenther A., Milam D., Newnam B.: Appl. Opt. 22 (20), 3276 (1983)

/20/ Guenther K. et al.: Appl. Opt. 23 (21), 3743 (1984)

/21/ Comley J.C. et al.: IEEE J. Quant. Electr. QE-17 (9), 1786 (1981)

/22/ Yamanaka C. et al.: IEEE J. Quant. Electron. QE-17 (9), 1678 (1981)

/23/ Mukherjee P., Kwok H.S.: Appl. Phys. Lett. 44 (2), 180 (1984)

/24/ Tajima T., Dawson J.M.: Phys. Rev. Lett. 43 (4), 267 (1979)

/25/ Katsouclas T., Dawson J.M.: Phys. Rev. Lett. 51 (5), 392 (1983)

/26/ Bunkenburg J. et al.: IEEE J. Quant. Electron. QE-17 (9), 1620 (1981)

/27/ LLL Annual Report UCRL-50021-83, section 2, pp. 2-5

/28/ Martin W.E. et al.: IEEE J. Quant. Electron. QE-17 (9), 1744 (1981)

/29/ Pellegrini C.: The Challenge of Ultra High Energies - Proc. of the ECFA-RAL Meeting, Oxford Sept. 1982, p. 249

/30/ Loewenthal D.D. et al.: IEEE J. Quant. Electron., QE-17 (9), 1861 (1981)

/31/ Moody St. et al.: IEEE J. Quant. Electron. QE-17 (9), 1856 (1981)

/32/ Sandström R.L., Levatter J.I.: CLEO'83, Techn. Digest, paper WF 2, p. 100, May 17-20, 1983, Baltimore /Md.

/33/ Smilanski I., Byron S.R., Burkes T.R.: Appl. Phys. Lett. 40, 547 (1982)
" - ": CLEO'83, May 17-20, 1983, Baltimore /Md., Techn. Digest, paper FE 4, p. 22

/34/ Corkum P.G., Taylor R.S.: IEEE J. Quant. Electron. QE-18 (11), 1962 (1982)

/35/ Taylor R.S. et al.: IEEE J. Quant. Electron QE-19 (3), 416 (1983)

/36/ "Excimer Lasers", ed. Ch. K. Rhodes, Springer Series "Topics in Applied Physics", Vol. 30, Springer Verlag, Berlin · Heidelberg · New York, 1979

/37/ Egger H. et al.: Appl. Phys. Lett. 41, 1032 (1982)

/38/ Szatmari S., Schäfer F.P.: Opt. Commun. 48 (4), 279 (1983)

/39/ Rokni M., Jacob J., Mangano J.: Phys. Rev. A 16, 2216 (1977)

/40/ Rutherford Appleton Laboratory, Annual Report 1982, Ch. 2

/41/ Rutherford Appleton Laboratory, Annual Report 1983, Ch. 2

/42/ Zeldovich B.Ya., Popovichev V.I., Ragulskiy V.V., Faizullov F.S.: Sov. Phys. JETP 15, 109 (1972)

/43/ Nosach O.Yu., Popovichev V.I., Ragulskiy V.V., Faizullov F.S.: Sov. Phys. JETP 16, 435 (1972)

/44/ Eidmann K., Sigel R.: Int. Conf. on Laser-Matter Interaction, Marly-le-Roi /France, 9-13. October, 1972

/45/ Eidmann K., Sigel R. in "Laser Interaction and Related Plasma Phenomena", ed. H.J. Schwarz and H. Hora, Plenum Press, Vol. 3B, 667 (1974)

/46/ Horn D.T.: Optical Engineering 21 (2), 252 (1982)

/47/ Murray J.R. et al.: IEEE J. Quant. Electron QE-15, 342 (1979)

Discussion

R. Palmer, BNL

I want to remind you that at least in some cases the specifications for laser powered acceleration are really very, very far from the specifications for fusion studies. The things that we have been looking at are, say, 3 ps CO_2 laser pulses, where an entire accelerator going up to several TeV would not require more than something like a 1000 joules a pulse. So that when you talk about already having tens or hundreds of kilojoules and wanting to go higher, I have to remind you that at least in some cases that is far above what we want. In another way we are far from having what we want, because we want to run at something like a kiloherz instead of once every ten minutes. We want high efficiency much more than capital cost. For instance if I calculate from your beautiful formula what the cost of a thousand joule laser would be I would come to only 10^7 deutschmarks, which is of course a bargain. On the other hand when I say that I want it to run at a kiloherz you are going to take back that offer.

Answer

This is certainly true. The lasers which I have been talking about are single pulse lasers. I do not think you can get a kiloherz with the kind of lasers which are now used for fusion studies. You would need a laser which is pumped differently.

R. Palmer

I've been talking to people who were interested in isotope separation and there are a number of kiloherz lasers about in the States which could be modified to work at CO_2 wavelengths. In fact when you discuss with these people they can imagine a 3 cm aperture providing something like 10 joules at a kiloherz for a not completely ridiculous cost and efficiencies which could be as high as 10%. So the story I get from the isotope separation people does not discourage me completely although the laser to the necessary specification does not exist. One of the reasons why they believe that it may be possible is that by operating at 10 atmospheres you exhaust the energy from all the lines simultaneously so the efficiency is much higher than you get from a nanosecond pulse.

Answer

But you should not overlook that such a laser cannot be operated in saturation; it will be small signalled. So the gain which is due to the line broadening is partially offset by the decrease in efficiency.

K.W. Chen, Texas

To increase laser repetition rate, I believe that high power magnetic switching can be used. Could you comment on this?

Answer

This could indeed be used but so far I do not know of any laser where it has been employed. It is certainly a possibility which should be exploited.

Remark

Magnetic switches have been operated at several hundred Hz at companies such as MSNW. Also at Los Alamos there is work on laser switching.